2006:317 CIV

MASTER'S THESIS

Measurement Prediction and Control of Steel Flows in the Casting Nozzle and Mould

Linda Bergman

Luleå University of Technology

MSc Programmes in Engineering
Chemical Engineering
Department of Chemical Engineering and Geosciences
Division of Process Metallurgy

2006:317 CIV - ISSN: 1402-1617 - ISRN: LTU-EX--06/317--SE

Abstract

Continuous casting is the dominating process to cast steel. Liquid steel is continuously fed from a tundish to a mould through a casting nozzle. The flow conditions in the mould are influenced by the flow pattern inside the casting nozzle as well as the level of steel in the tundish. The flow into the mould is regulated by a stopper rod or a slide gate. The surface of the strand solidifies quickly in the mould and it is important to maintain a constant level of steel to avoid surface defects.

A new physical model that simulates continuous casting has been developed. A physical model of this type is unique. The scale of the model is a commonly used full-scale casting machine at slab casters, except the dimension of the tundish. It is possible to generate different types of flow conditions at simulation in the model.

Water and liquid steel has similar kinematic viscosity and water is therefore often used for simulation of the continuous casting process. This simulation has been performed using an alloy with a low melting point. The alloy has besides the low melting point, similar physical properties as steel.

Measurements with a compact laser vibrometer have been performed to examine the possibility to quantify the volumetric flow of alloy in the model. The compact laser vibrometer measures the vibrations on the surface of the casting nozzle as the alloy flows through during simulation.

The flow of alloy in the model is determined by the velocity of the pump. A calibration of the pump was done to specify the volumetric flow at a specific pumping velocity. This provides the possibility to examine the signal from the sensor during controlled circumstances.

The investigation was performed during simulation at specific single phase flows. It was found that the compact laser vibrometer shows a trend of increasing frequency at higher flow rates. A background noise was created by the engine of the pump and measurements were done to be able to exclude this type of disturbance.

Acknowledgement

This report is the result of measurements done with a compact laser vibrometer in a physical model, which simulates continuous casting. An alloy with low melting point was used to simulate steel. The project has been very interesting to work with and I have learnt a lot during this part of my education.

The project was performed at MEFOS, Metallurgical Research Institute AB which is an industrial research institute for the metallurgical and metalworking industry. MEFOS has unique large scale pilot plant equipment and the company is well known world-wide because of their ability to perform very large research projects.

Five years have past since I've started my education at Luleå University of Technology. I am appreciative to a lot of people who have helped, and inspired me during this time.

Firstly, I will like to express my appreciation to Anita Djärv, who developed my interest in chemistry. Secondly, my greatest thanks to my supervisors Johan Björkvall at MEFOS and Bo Björkman at the department of process metallurgy, LTU.

There have been many people involved in this project, but I would like to send a special thank you to; Christer Olofsson, Ulf Sjöström and Seymour Eriksson for helping me with knowledge of the process, analysis and measurements.

Finally, my greatest hugs to Martin, my family and friends for being so supportive during these years of education.

_____

Linda Bergman 2006-10-30

Table of contents

1 Introduction

1.1 Background

The production of steel from primary raw material occurs mainly through the blast furnace process. Iron ore, coke and slag formers are fed at the top of the furnace and hot metal is tapped from the bottom. Hot metal is transported to the steel works where a lowering of the amount of sulphur takes place. The amount of carbon is thereafter reduced in a converter and steel is produced. A final adjustment of the steel produced is further performed in a ladle metallurgy step.

Steel produced from secondary raw material is melted in electrical furnaces. Scrap and slag formers are charged and melted in the furnace which also works as a converter to lower the amount of carbon. The ladle metallurgy step is thereafter performed.

The ladle metallurgy step is the final modification of the produced steel. Adjustments of alloys and the amount of carbon are adjusted here. Casting occurs after this process step. 60 % of the worlds steel production is cast in a continuous process. In Asia and the western European countries is this number over 80 %. Continuous casting machines have been developed since 1940: s. The continuous casting process has lead to advantages such as better strength and quality of the material, less consumption of energy and a higher productivity [1].

Liquid steel is continuously fed from a tundish to a mould through a casting nozzle during continuous casting. The mould is cooled and steel solidifies successively to a homogenous strand. The geometry of the strand is adjusted by the dimensions of the mould and is in continuous casting defined as billets, blooms or slabs.

The level in the mould is controlled by the height in the tundish and a regulating device, such as a stopper or a slide gate. It is important to have good process control to avoid surface defects on the cast products. A gas is normally injected down the casting nozzle. This influences the flow pattern in the nozzle and thereby the level in the mould. The flow through the nozzle can change due to clogging and wear.

1.2 History

Sir Henry Bessemer, England, was the first person who presented the idea to cast steel continuously. The method to cast thin slabs was suggested in 1850 and the first attempts were done in a pilot plant 1943 in Germany. The first commercial equipment came into operation about 20 years later. Continuous casting is a complex process where the steel fed into the tundish has to be correlated with the casting velocity. The continuous casting process led to an increase of productivity and was thereby a commercial breakthrough. The quality of the slabs and the economy of the process were found to be much better than ingot casting, which was the main process at that time and the process developed therefore quickly.

Vertical machines were used in the beginning. Slabs with a coarser cross section were cut in vertical position and slabs with a thinner cross section were bend and straightened before they were cut in the horizontal direction.

The casting velocity should be high in order to keep a high productivity. This led to long slabs before they were cut off. Vertical machines in the process plant led to very high buildings and an introduction of bent machines were done to be able to solve this problem. The bent machines led also to reduce the investment costs. Different types of machines are illustrated in figure 1 [2-3].

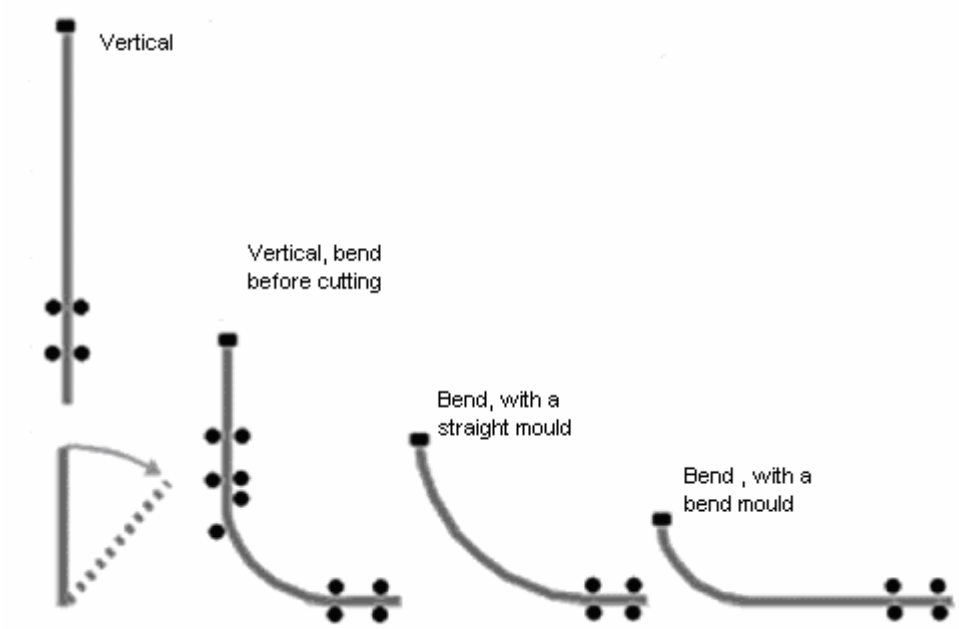

Figure 1. Examples of continuously casting machines. The height of the building can be reduced to the right as the height of the machine decreases [2].

1.3 Aim of the project

Today, mass balances are the basis for calculation of flows at casting. There is a need to quantify the flow and foresee disturbances in the process. Continuous casting is a high temperature process and a great benefit is therefore the use of non-contact sensors.

A physical model with an alloy of low melting point was used. The model simulates the process of continuous casting and an alloy with low melting point simulates steel. The model makes it possible to examine signals from sensors at temperatures lower than the actual process.

A method to measure the flow in the casting nozzle and mould would lead to an indication of product quality and also to indications of disturbances in the process, such as clogging and wear.

2 Theory

2.1 Continuous casting

A final adjustment of the steel is performed at the process step of the ladle metallurgy. Ladles are transported to the continuous caster to support the casting machine with steel. A cross section of a continuous caster can be seen in figure 2. Steel is continuously fed from a tundish to a mould through a casting nozzle.

During the time it takes to empty a tundish, the consumed ladle is replaced with a new one. The level of steel in the tundish and in the mould is controlled with a valve, usually a slid gate or a stopper rod. The wear of the lining in the tundish, on the stopper and of the casting tube determines the number of ladles which are cast in sequence [2-4].

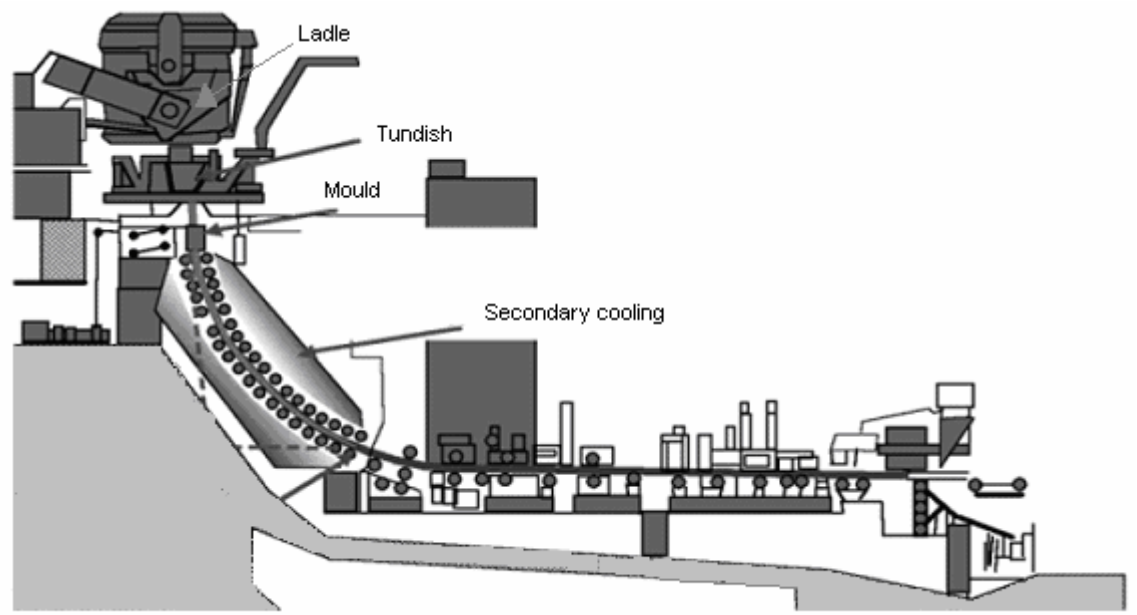

Figure 2. Cross section of continuous casting machinery. A ladle is delivered from the secondary steelmaking process with liquid steel. Steel runs through a ladle shroud down to a tundish and further down in the mould [3].

Liquid steel is easily oxidised in contact with oxygen. The ladle is usually covered with a lid and the surface of the steel in the tundish is covered with a powder to avoid contact with the atmosphere.

A tundish is an important link during casting and acts for instance as a slag separator and a buffering system during changes of ladles. It forces the casting beam into a proper position and control the flow of steel into the mould with help of a regulating system.

The slag separation in the tundish is enhanced by a long residence time and thereby a big tundish. The optimal size of a tundish is chosen to get a residence time of about four to five minutes due to the fact that a too big one is not realistic.

The height of steel in the tundish is also an important parameter as a high level of melt leads to a longer residence time than a low. A low level of steel in the tundish will also risk that already separated slag is drawn into the bath again. The level of steel in the tundish influences the level of steel in the mould.

A mould length varies from about 500 to 900 millimetres and casting velocities varies with dimensions of the mould. The mould oscillates to reduce the friction between the solidifying shell and the wall of the mould and enhances thereby the rejection of the strand out of the open bottom. A mould is the primary cooling step in continuous casting. Liquid steel is immediately solidified at the surface due to a very fast heat transfer through the water chilled copper mould. The thickness of the shell is increased down the length of the mould due to the intense cooling.

To prevent an oxidation of the steels surface in the mould, casting powder is added. The inner surface of the powder is in contact with steel and melts meanwhile the outer surface is intact and acts as a lubricant between the solidifying shell and the oscillating mould. The molten inner surface of the powder makes it possible to attract inclusions [2-4].

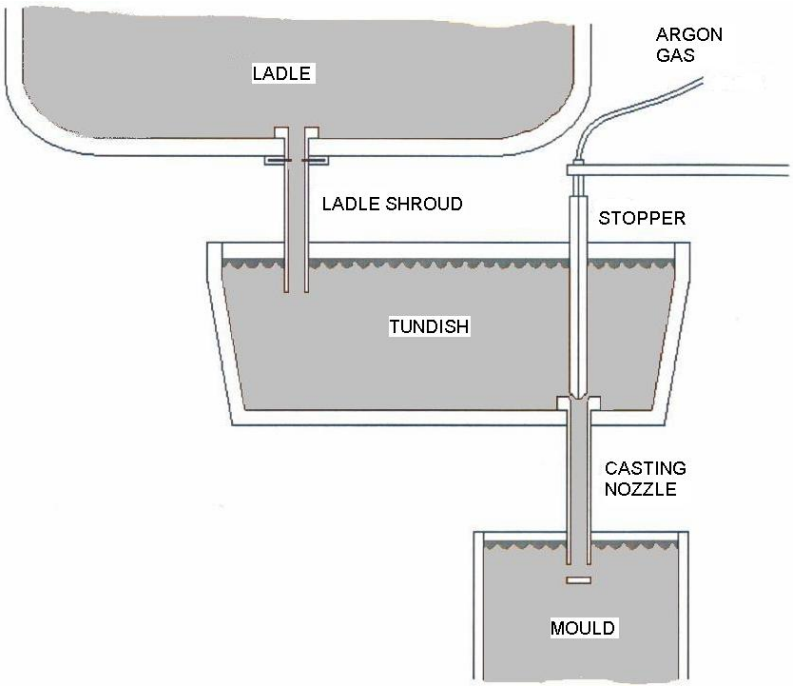

Figure 3. Cross section of ladle, tundish and mould [1].

The mould oscillates to prevent sticking of the solidifying shell on the mould. This means that the mould has a sinusoidal movement at a frequency that provides negative strip. The mould moves downward faster than the solidifying skin for a percentage of the oscillating cycle and avoids thereby steel to stick on the copper surface. Casting powder has to be provided here as an interface between the solidifying skin and the copper plate to act as a lubricant. Casting powder in contact with liquid steel melts to form a slag, which infiltrates into the gap between steel and copper at the meniscus. There are different kinds of lubricants depending on for instance composition of the steel.

When the solidified skin is thick enough to withstand the ferrostatic pressure of the liquid steel inside the strand, it leaves the mould and is further cooled by water sprays. This is called the secondary cooling. Rollers supports the strand until it is completely solidified, it would otherwise become bulged because of the pressure from the liquid steel inside of the strand. The strand is cut into smaller dimensions at a slitting station and further treated by for instance rolling.

2.2 Quality

There are several factors that influence the quality of the slabs and have to be controlled.

The temperature in tundish is around 30˚C above melting point of the steel. Temperature variations can be limited if the tundish is preheated and other efforts are made to reduce the temperature losses from the tundish.

The conical shape of the mould is important for the primary cooling from the mould wall. If the solidified shell has a close contact with the wall, the cooling will be effective. A shrinking of the material occurs during cooling. The shrinking shell can in the beginning be compensated by the ferrostatic pressure of the liquid steel inside the strand. Liquid steel will force the shell against the mould wall and be further cooled. The shell becomes after a while so thick and strong that the shrinking can not longer be compensated by the pressure from the melt. A conical profile of the mould makes it possible to follow the shape of the solidifying steel as cooling shrinkage occurs. Cooling in the mould is affected if the mould is worn. A poor contact creates a gap of air and cooling will be reduced.

The flow of the water in the primary and secondary cooling is important to keep an even cooling rate. An uneven growth of the shell could otherwise take place.

It is important to have the right flow of steel into the mould to keep a constant level. This is regulated by the surface level in the tundish together with the size of the gap between stopper and casting nozzle.

Important quality problems in continuous casting are centre segregations, surface defects, inclusions and cracks [2-4].

2.2.1 Inclusions

Oxidised particles have a lighter density than steel itself. Inclusions that not are separated before casting can be trapped during the solidification process down the strand.

One cause of macro slag inclusions is casting powder that can be drawn into the steel. Even if a good separation of oxides have been done in the ladle, it is important to optimise the separation in the tundish and mould. Inclusions should be separated before the tundish is reached. This is not practically possible. A large tundish leads to a longer residence time and enhances the rejection of inclusions. Stirring is positive and it can be helpful to insert baffles into the tundish to prolong the way from inlet to outlet. It is important to cover the surface and to use a powder that has the ability to attract inclusions and solve them.

Inclusions can stick to the wall of the outlet of the tundish and in the casting nozzle. A framework of inclusions will be built and a retardation of the flow will occur. Smaller dimensions of the outlet are more sensitive than larger. The most common inclusion creating clogging is alumina. One way to reduce the problem is to add Si-Ca to modify the inclusions and get them liquid. A good separation of the Al_2O_3- clusters before starting a casting will also reduce the problems [2-3].

If possible, the height between tundish and mould should be limited to restrain the penetration of the jet down to the mould. This can to some extent be restricted by the shape of the outlet ports in the casting nozzle, but the most effective way is probably to use an electromagnetic brake[1], which restricts the flow of the steel into the mould.

2.2.2 Cracks and surface defects

When the strength of the steel is exceeded at a certain temperature, local tensions arise and cracks occur. Both internal and surface cracks can occur. Figure 4 shows different examples of cracks. When cracks is received in production, it can be hard to tell if it primary depends on a reduction of strength or a locally increased tension.

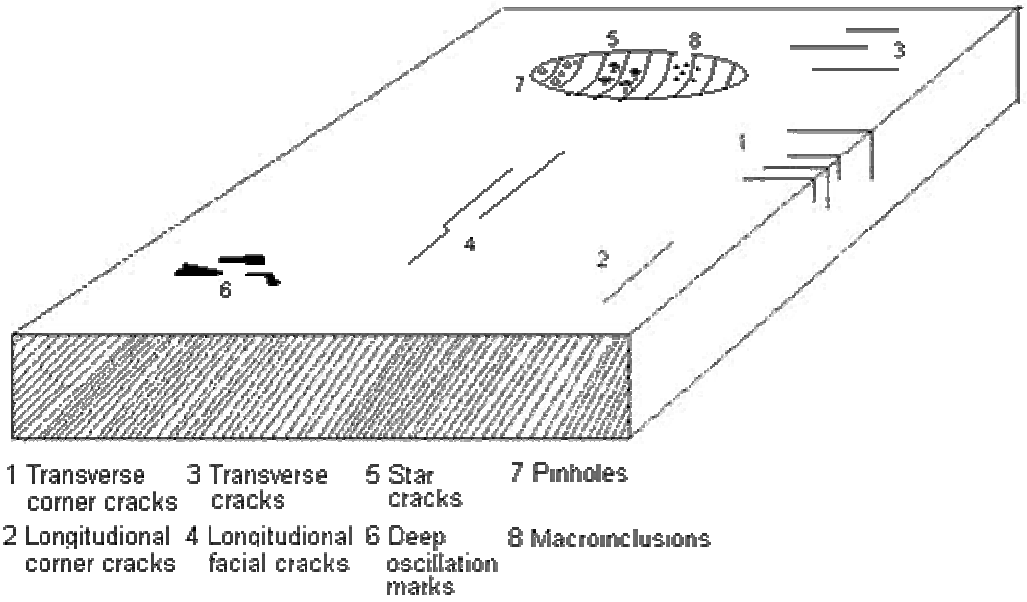

Figure 4. Different types of surface defects and cracks on a continuously cast slab [3].

With a correct design and construction, the margin towards crack formation increases. For instance, rounded corners of a slab will naturally give better possibilities than sharp edges due to a slower cooling. A sharp straightening of a bend strand should also be avoided because tensions from straightening of the strand could otherwise cooperate with locally raised tensions to create transverse cracks.

[1] EMBR: Electromagnetic brake process. This consists of two sets of coils placed along the outer walls of the mould faces. The magnetic field reduces the liquid steel velocity and the impurities float to the surface where they are trapped by the mould powder.

The variation in tension, which leads to outer cracks, can arise in the primary as well as the secondary cooling because cooling-rate is high in both positions. A shell is fast created in the mould and this is also cooled very quickly.

Examples on factors that can lead to disturbances of shell growth in the mould are:

- Variations of the steel level as well as a worn mould or incorrect conical shape
- Unsuitable casting powder, variation in the film thickness, or a disturbed flow
- Incorrect oscillation movement

The surface of the solidifying strand is formed in the mould and consequently the bulk of surface defects are related to mould technology. Variation of the meniscus level can have a significant effect on the quality of the strands surface as it is formed. The teeming system of the tundish is used to control the steel flow to maintain a constant level in the mould [2-4].

3 Flow in continuous casting

3.1 Mould level control

A regulating system that controls the flow of steel from the tundish to the mould is needed to maintain a constant level of steel in the mould. The meniscus level in the mould has a strongly effect on the appearance of surface defects on the cast products. The flow in the actual mould will also have a strong effect on the source of defects in the final product.

The steel flows from the tundish to the mould through a submerged entry nozzle, SEN. The connection between the submerged entry nozzle and the tundish has to be gas-and air tight to prevent oxidation of liquid steel [5].

The submerged entry nozzle has an important influence on steel quality through its effect on the flow pattern in the mould. It should deliver steel uniformly into the mould while preventing problems such as surface waves, meniscus freezing and crack formation [8].

As the strand solidifies, it is continuously withdrawn from the bottom of the mould at a rate, casting speed which matches the flow of the incoming metal. The flow through the nozzle is driven by gravity; due to the difference in pressure between the liquid levels of the mould and tundish top free surfaces. Thus, the flow rate depends upon the amount of steel in the tundish and the flow characteristics inside the submerged entry nozzle [8].

The flow of the steel from the tundish to mould is controlled either by a sliding gate mechanism or by a stopper rod device, which is mounted at the inside of the tundish [5]. When a stopper rod is used, it is pushed down through the tundish to partially plug the exit. The slide gate mechanism blocks off a portion of the submerged nozzles pipe section by moving a disk-shaped plate through a horizontal slit across the entire nozzle [8]. As the stopper rod is more common in Europe [5] this has been chosen as the focal point of this report.

In order to ensure good steel cleanness and provide sufficient operation life it's important to choose suitable materials for the entry nozzles. The entry nozzles have to withstand the chemical attack of alloying elements such as aluminium, sulphur, manganese as well as slag from the casting powder in the mould.

Figure 5 shows the cross-section of a stopper rod and a submerged entry nozzle. A stopper rod defines the rate of flow of the molten steel by the relative position of the stopper head to the seat of the tundish nozzle. Optimization of control is achieved through the complementary geometries of the stoppers head and nozzle seat. There is a wide variety of stopper head profiles, each having different degrees of sensitivity and controllability of steel flow to meet the wide range of customer requirements. A stopper with a hemispherical head will be considered in this report.

When casting aluminium-killed steels, nozzle clogging can occur due to alumina adhering to the submerged entry nozzle material. As seen in figure 5, the stopper rod is hollow rendering the possibility to inject argon gas and thereby reducing the occurrence of nozzle clogging.

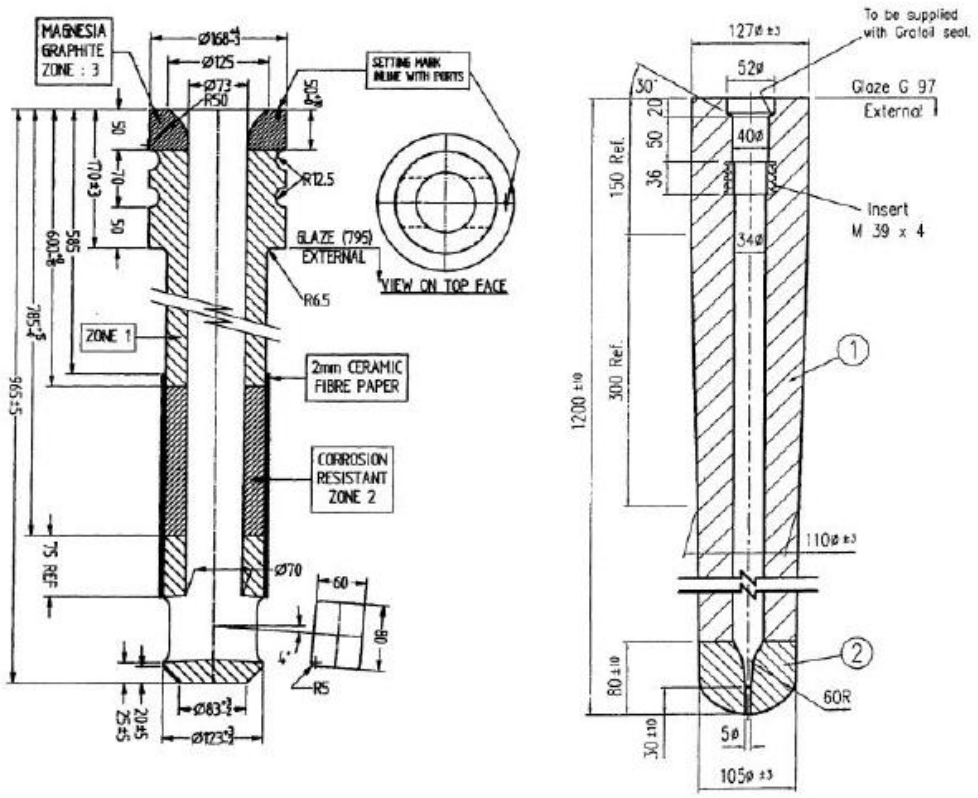

Figure 5. Cross section of an entry nozzle to the left and a stopper rod to the right

The control of the steel flow is effected by the dimensions of the submerged entry nozzle and stopper head as well as material selection and argon injection. Nozzle clogging can be minimized and operation time of the submerged entry nozzle can be extended by optimizing these parameters. A key characteristic for any combination of stopper rod and entry nozzles is the relationship between steel flow rate and the vertical stopper position [6]. Steel flow is regulated from tundish to mould by variation in stopper lift. When stopper lift position changes, the open area between the stopper and nozzle seat is also changed [6-7].

The construction of a submerged entry nozzle is of great importance. A submerged entry nozzle should be constructed to deliver steel in an optimum way through its ports, preventing surface turbulence and shell erosion. Plant observations have found that many serious quality problems are directly associated with the operation of the submerged entry nozzle and the flow pattern in the mould. This will for example be surface waves and turbulence near meniscus which lead to entrapment of slag or gas bubbles into the steel, causing large inclusions and surface defects. Clogging is an example where clusters of inclusions grows on the walls of the submerged entry nozzle and redirect the flow. Clogging will thereby also effect the jet characteristics exiting from the ports of the submerged nozzle [8].

Najjar et al [8] discusses the design of the nozzle and its importance. Optimum designs of the ports are needed to avoid both shallow and deep angles of the jet, according to the mould width, casting speed, and other casting conditions.

A shallow mean jet angle may result in a delivery of the molten steel directly to the meniscus. This can result in surface turbulence and thereby entrapment of slag in steel. A disruption of solidification near the meniscus will occur and this is critical to surface quality [8].

A steep jet angle may deliver the steel too deep into the mould and slow down the flotation of inclusions and thereby their removal by the slag layer. It may also cause the molten steel to lose its superheat by the time it reaches the meniscus. This promotes freezing of the meniscus, which may cause deep oscillation marks, poor quality and even so called bridging where the top surface of the steel freezes across the distance between the entry nozzle and the wide face of the mould.

A high speed of the molten jet towards the solidifying shell can result in shell erosion in local spots and thereby be a potential source for breakouts. High speed flow from the nozzle will also inhibit the flotation of inclusions and argon bubbles and will thereby lead to serious surface defects in the final product.

Finally, temporary variations of the flow that enters the mould may cause surface turbulence, rapid surface level fluctuations, sloshing, and entrainment of mould slag into the liquid steel.

3.1.1 Nozzle clogging

Nozzle clogging is one of the most disruptive phenomena in the operation of the tundish-mould system in continuous casting of steel. Tundish nozzle blockage is related to the presence of non-metallic particles in liquid steel. These particles precipitate and/or are collected in the bore of the submerged entry nozzle [9].

When casting aluminium-killed steels, nozzle clogging can occur due to alumina adhering to the submerged entry nozzle material. To reduce the occurrence of nozzle clogging, argon gas is injected down the stopper rod.

Product quality is in several ways affected negatively by nozzle clogging. Flow pattern in the mould is usually designed based on the assumption of no clogging and clogs can change this pattern. Mould level variations and unstable flow in the mould are more severe with clogging. Another problem which can arise from clogging is that a nozzle clog breaks off and enters the flow stream. This leads to seriously problems with the internal quality. Clogs get trapped in the solidifying steel and form inclusion defects that drastically lower strength and toughness. Even if it is not entrapped in the solidified steel, a large clog can be detrimental if it suddenly floats into the slag layer [10].

Alumina in clogs that breaks off can disrupt the local slag composition and increase slag viscosity. This can lead to a more difficult slag infiltration at the meniscus. Surface defects such as longitudinal cracks can thereby arise.

As the build-up proceeds, the opening between the stopper and nozzle seat must increase to maintain the desired flow rate. When the opening to the submerged entry nozzle reaches its maximum position, production must stop and the nozzle must be replaced. It is very important to find and understand ways to both detect and prevent clogging [10].

3.2 Argon injection

The principal method which is utilized to improve problems with clogging in the submerged entry nozzle is the introduction of gas into the system. Heaslip et al [9] describes the possible mechanisms by which clogging is reduced as the result of gas introduction;

1. The flow system is pressurised and this minimises reoxidation that can arise due to air aspiration.
2. The refractory get coated by a gas curtain and metal is thereby prevented to be in contact with the walls.
3. The gas provides a flushing action to remove adherent particles from the refractory.

Guy et al [11] discuss that several developments such as dams, weirs, filters and argon bubbling have been tried out to improve constant flow rate, low inclusion count, temperature close to liquidus and a constant chemical composition. He explains that argon bubbling through the stopper rod can solve three out of these four requirements due to the fact that argon bubbling provides a homogenization effect which leads to a rather constant temperature and chemical composition. It will also stimulate a flotation of inclusions which means that inclusions attach to the argon bubbles and the inclusion count will therefore be low.

The elimination of inclusions in steel by argon bubbling is enhanced by two phenomena:

1. Soft stirring of liquid metal, avoids short residence time of the metal in the tundish and promotes inclusions flotation.
2. Attachment of inclusions to the bubbles. The smaller the bubbles, the higher the attachment efficiency.

The injection of argon gas will affect the flow pattern in the submerged entry nozzle, and subsequently in the mould. Some bubbles may attach with small inclusions and become entrapped in the solidifying shell, resulting in pencil pipe and blister defects on the surface of the final product. Bai [10] discuss some other disadvantages with argon injections and points out that it is important to optimize the argon injection to the minimum amount needed to achieve its benefits.

Heaslip et al tried different injection sites in a water model and pointed out that conditions of strong stable suction were found to exist at the bottom of the stopper rod, making this an optimum site for injection [9].

3.3 Two phase flow

Two phase flows refers to flows where two phases are present. It can for instance be solid slag inclusions and metal, or metal and gas. A two phase flow of gas and liquid will normally occur through the submerged entry nozzle in continuous casting due to the argon injection down the stopper rod.

3.3.1 Upward co current flow in vertical pipes

Figure 6 shows regimes that are obtained in vertical, upward co current flow at different gas and liquid flow rates. The ratio of gas to liquid flow rate is increased to the right.

The bubble regime, to the left in figure 6, shows various sizes of bubbles that are dispersed throughout the liquid. The size of the bubbles increases when the flow rate of gas increases. Bubbles can have some tendency to concentrate towards the centre of the pipe.

As the gas flow is further increased, there will be a point when many bubbles coalesce to produce slugs of gas. So called Taylor bubbles are formed. They are large, and have a diameter that is nearly equal to the diameter of the pipe and being recognized by their spherical noses. Liquid surrounds the bubbles with a thin film, but is also found between the Taylor bubbles, containing some small bubbles. Taylor bubbles do not attach to the wall of the pipe.

At higher flow rates, a chaotic type of flow, generally known as churn flow is established. Churn flow has irregularly shaped portions of gas and liquid in a churning motion over almost the entire cross section of the pipe.

A further increase in the gas flow rate causes a separation of the phases. Liquid will mainly be flowing on the wall of the tube and gas in the core. Liquid droplets are carried by the gas in the core. The main difference between the wispy-annular and the annular flow regimes are that in wispy-annular, the entrained liquid in the core is present as relatively large drops and the liquid film against the wall contains gas bubbles , while in the annular flow regime the entrained droplets in the core do not coalesce to form larger drops [12-13].

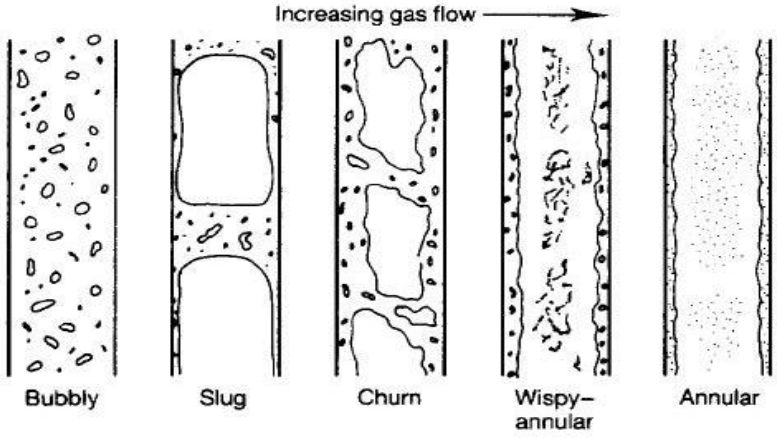

Figure 6. Flow regimes for upward two phase flow in vertical pipes [12].

3.3.2 Downward co current flow in vertical pipes

Six different flow patterns are confirmed in piping handbook [14] for downward co current flow in vertical pipes, figure 7.

The downward bubbly flow structure is quite different from the upward bubbly flow configuration. Bubbles are spread over the entire cross section in upward bubbly flow, whereas in the downward flow, bubbles gather near the pipe axis. This coring effect is similar to the phenomenon observed in a flow of liquid loaded with solid particles whose density is smaller than the liquid density [14].

When the gas flow rate is increased and the liquid flow rate is held constant, the bubbles agglomerate into large gas pockets. The top of these gas plugs is dome shaped whereas the lower extremity is flat with a bubbly zone underneath. This slug flow is generally more stable than in the upward case.

The annular configuration can exhibit several aspects. For small liquid and gas flow rates, a liquid film flows down the wall, a falling film flow. If the liquid flow rate is higher, bubbles are entrained within the film and refer to a bubbly falling film. When liquid and gas flow rates are increased a churn flow appears, which can evolve into a dispersed annular flow for very high gas flow rates.

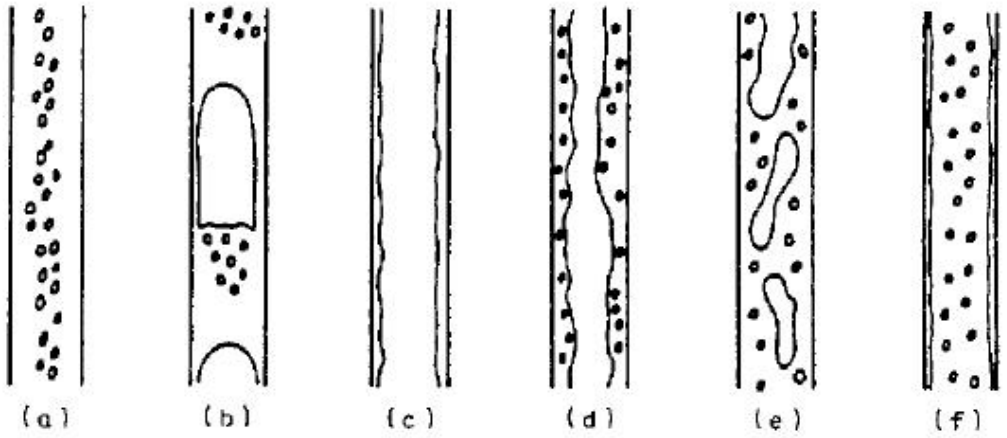

Figure 7. Downward co current two phase flow in vertical pipes; a) bubbly flow; b) slug flow; c) falling film flow; d) bubbly falling film flow; e) churn flow; f) dispersed annular flow [14].

As the result of buoyancy, the bubbles ascend to the surface of the liquid after they leave the nozzle entry. Due to the effect of the surface flow, the floating bubbles are more close to the nozzle. The trajectory of the bubble is affected by the bubble diameter and the molten steel flow, and the diameter is dominant [19].

Lei et al [19] write also about variations of surface oscillation with gas flow rate during different casting speeds. It is shown that the oscillation near the meniscus becomes larger as the casting speed increases. The probability of slag entrapment will thereby be higher. It is also shown that with increasing flow rate, the impinging position of steel flow at the narrow face moves upward and the oscillation near meniscus becomes more unsteady due to the increase of the number of bubbles in the mould.

Without argon injection in the mould, the molten steel velocity near surface and meniscus oscillation increases with the augment of casting speed, so slag entrapment occurs more easily. However, the correlation between slag entrapment and casting speed changes if argon injection is used. With the increase of casting speed bubbles penetrate more deeply into the mould.

Depending of flows of steel and argon gas one can get different flow pattern in the submerged entry nozzle and thereby affect the level in the mould. A large quantity of gas in relation to quantity of steel gives an annular flow. The optimal flow pattern in continuous casting is a bubbly flow to achieve a stable meniscus and also achieve the benefits with the injected gas.

3.3.3 Flow pattern in a submerged entry nozzle

A metal in its melted state can be considered a fluid. Even though it can be large changes in pressure, there are small density differences and flow of molten steel can thereby be referred to as incompressible flow.

In the continuous casting of steel, control of delivery of molten steel through the submerged entry nozzle is critical in order to ensure the stability of the meniscus and create the optimum laminar flow patterns. It is important to have a laminar flow in the mould to ensure a stable meniscus. The type of flow in the submerged entry nozzle influences the surface quality and thereby also the value of the cast product. There are several factors that influence the stability between the tundish and mould and some of them are metal level in tundish, mass flow rate, diameter of the nozzle, flow rate of argon gas and of course clogging in stopper and nozzle.

Xiandong et al [17] describes typical examples of two phase steel flow patterns within a submerged entry nozzle, figure 8. The optimal bubbly flow, where argon bubbles travel with the stream, can be seen to the left. The central stream, in the middle, is the flow in transition to annular flow. Annular flow is viewed to the right in figure 8, where a stream of metal with a central gap of gas can be seen. This type of behaviour will coincide with the earlier discussion of a central air gap of the annular flow of liquid and air flowing in a vertical pipe. It is possible to change flow pattern during casting, depending on the flow rates of steel and gas.

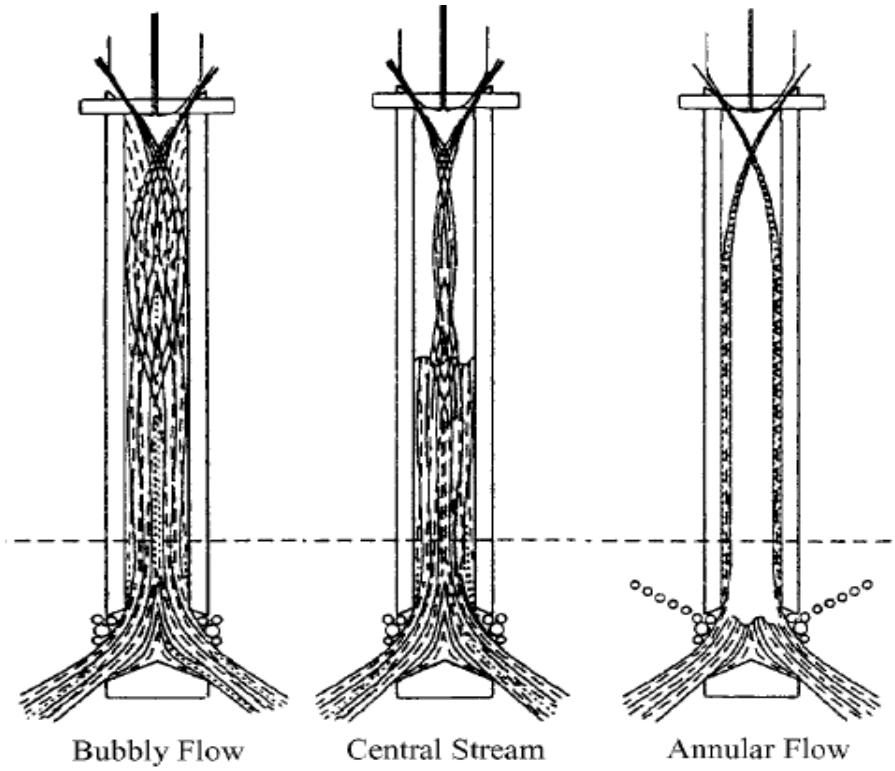

Figure 8. Typical examples of steel flow patterns at casting in a submerged entry nozzle [17].

Heaslip et al [9] did observations of fluid flow in a water model with a stopper rod control. When he used gas injection down the stopper rod, gas was drawn into a vortex which formed around the end of the stopper. This diminished in the submerged entry nozzle and there was a uniform distribution of gas across the entire tube diameter. There was not any sign of back mixing and nearly parallel lines could be seen inside the tube. The flow was seen to proceed in a plug-like manner from top to bottom with a little influence of radial position and there was symmetry around the tube axis. This behaviour was in the investigation independent of casting speed.

3.4 Physical modelling

To consider a situation that occurs at the process plant in a laboratory, a prototype of the real machine has to be made. To be able to simulate the real process, there are some criteria that have to be full-filled.

3.4.1 Criteria for modelling

For a model to describe a real situation well we must ensure quality of the dimensionless numbers. The ratio of various forces occurring in mixing vessels can be expressed by the dimensionless numbers, which in turn serve as similarity parameters for scale up of mixing equipment.

The importance to achieve geometric, kinematic and dynamic similarity for two systems was studied in chemical engineering [20] and refers to;

- *Geometric similarity* prevails between two systems of different sizes if all counterpart length dimensions have a constant ratio.

- *Kinematic similarity* exists in two geometrically similar units when the velocities at corresponding points have a constant ratio. Also the paths of fluid motion, flow patterns, must be alike.

- *Dynamic similarity* occurs in two geometrically similar units of different sizes if all corresponding forces at counterpart locations have a constant ratio. It is necessary here to distinguish between the various types of force: inertial, gravitational, viscous, surface tension and other forms. Some or all of these forms may be significant in a mixing vessel.

Dynamic similarity is a necessary criterion for modelling. Generally we are balancing force ratios between the model and the prototype to maintain similitude. Dynamic similarity ensures that interactions between the forces which occur in the model will also occur in the same fashion in the actual system [16].

Kinematic and dynamic similarities both require geometrical similarity, so the corresponding positions can be identified in the two systems of laboratory and full scale equipment respectively.

Tritton [21] writes that dynamic similarity of two geometrical systems exists if they have the same value of the Reynolds number; If Reynolds numbers are the same for two geometrically similar situations the non dimensional pressure and velocities are the same. Hence, they have the same solutions and the same flow pattern occurs.

An early stage of the investigation of a new configuration is usually the formulation of non-dimensional parameters, which determines the dynamical similarity. Reynolds number is a general procedure to use. When other equations or other terms in the equations are applicable, other dimensionless combinations of the parameters may be formulated in addition to or instead of the Reynolds number. Reynolds number determines the nature of flow. The constancy of the ratios of other forces results for instance in the Froude number

Reynolds number is given by;

$$\mathrm{Re} = \frac{\rho * u * l}{\mu} = \frac{u * l}{\nu} \quad \textbf{(1)}$$

ρ = Density (kg/m^3)
u = Average velocity (m/s)
l = Length of pipe (m)
μ = Dynamic viscosity (Pas)
ν = Kinematic viscosity (Ns/m^2)

Tritton [21] describes further, that in certain circumstances waves can develop on a free surface. These waves are dominantly gravitational and in addition to u, l, ρ and v, the acceleration due to gravity, g, is a parameter of flow. There are two independent non dimensional combinations of these, Reynolds and Froude number.

Reynolds number was given in equation (1) and Froude number is given by;

$$Fr = \frac{u^2}{g * l} \quad \textbf{(2)}$$

u= velocity (m/s)
g=acceleration due to gravity (m/s^2)
l=length of pipe (m)

To achieve dynamic similarity between the two systems, it requires that;

$$\mathrm{Re}_1 = \mathrm{Re}_2 \quad \textbf{(3)}$$

$$Fr_1 = Fr_2 \quad \textbf{(4)}$$

Modelling of steel melts gives a useful insight to the flow phenomena in continuous casting. When a physical model is used, a reduced scale model can not simultaneously satisfy the Reynolds and Froude criteria. Sahai and Emi [16] describe that flow in a tundish is generally turbulent and Reynolds number similarity is very important in laminar flow but becomes less important in turbulent flow.

3.4.2 Model metal

The alloy that was used in the model is called MCP 137. Water is often used in physical models to simulate steel. The kinematic viscosity of water at room temperature is almost the same as molten steel at 1600˚C, within 10 % [16]. The alloy and the physical model provide a unique possibility to examine the compact laser vibrometer at temperatures lower than a continuous casting process.

MCP 137 is a eutectic mixture of 43 atomic % Bismuth and 57 atomic % Tin. It has a melting point of 137 degrees and its density is 8.58 g/cm^3,

The viscosity of the alloy can be estimated by calculation [15].

$$\eta = A * \exp\left(\frac{B}{R * T}\right) \quad \textbf{(5)}$$

$$A = \left(\frac{1{,}7 * 10^{-7} * \rho^{\frac{2}{3}} * T_m^{\frac{1}{2}} * M^{\frac{-1}{6}}}{\exp\left(\frac{B}{R * T_m}\right)}\right) \quad \textbf{(6)}$$

$$B = 2{,}65 * T_m^{1{,}27} \quad \textbf{(7)}$$

η = Estimated viscosity of alloy, Pas
ρ = 8580 kg/m^3
T_m = 137˚C
M = Molar mass, kg/mol
R = Gas constant, 8.3144 J/K*mol

The temperature at simulation is 165˚C and molar mass for Bismuth and Tin is 208.98 and 118.71 g/mol respectively. The alloy has thereby a molar mass of 0.158 kg/mol.

$$B = 2{,}65 * (137 + 273)^{1{,}27} = 5516{,}75 \text{ J/mol}$$

$$A = \left(\frac{1{,}7 * 10^{-7} * 8580^{\frac{2}{3}} * (137 + 273)^{\frac{1}{2}} * 0{,}158^{\frac{-1}{6}}}{\exp\left(\frac{5516{,}75}{8{,}3144 * (137 + 273)}\right)}\right) = 0.389 \text{ Pas}$$

$$\eta = 0{,}389 * \exp\left(\frac{5516{,}75}{8{,}3144 * (165 + 273)}\right) = 1.77 \text{ mPas}$$

The alloy has a conductivity of $1.0*10^6$ $(\Omega m)^{-1}$ at 165°C [23]. Liquid steel has a conductivity of $7.34*10^5$ [24]. The alloy has consequently a conductivity that is 1.4 times higher than liquid steel.

The binary phase diagram for Bismuth and Tin is schematically viewed in figure 9. The solid is a mixture of α- and β-phases, respectively the solid solutions of bismuth in tin and of tin in bismuth.

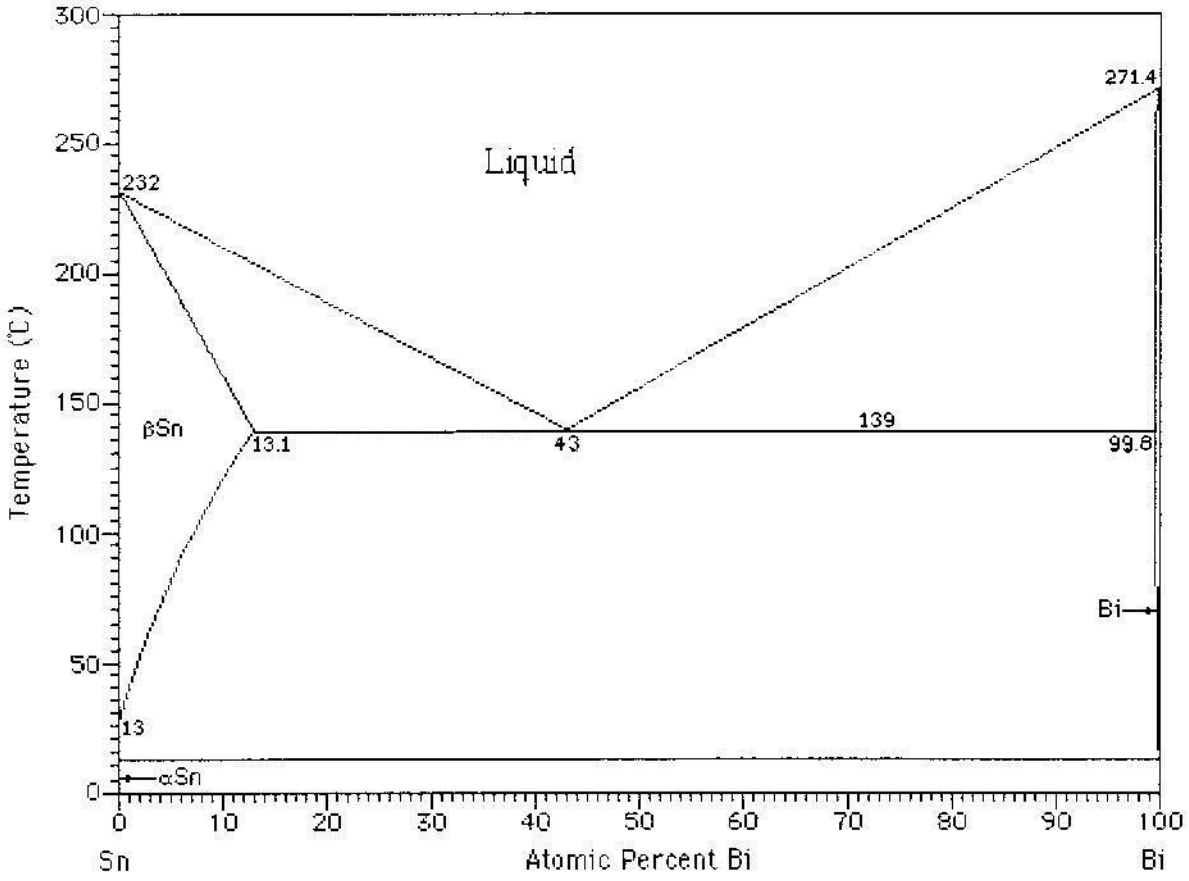

Figure 9. Binary phase diagram of Bismuth and Tin

3.4.3 Description of the physical model

The physical model consists of a tundish, casting nozzle, a mould and a pumping section. The model makes it possible to simulate continuous casting by pumping an alloy of tin and bismuth. The model is build of stainless steel and can be seen in figure 10. The scale of the model is a commonly used full-scale casting machine at slab casters. The only exception is the dimension of the tundish, which is a cylindrical tank. The casting nozzle is the same as used at normal production. The use of a low melting alloy in a physical model provides the possibility to investigate the compact laser vibrometer at specific flows and temperatures lower than the actual process.

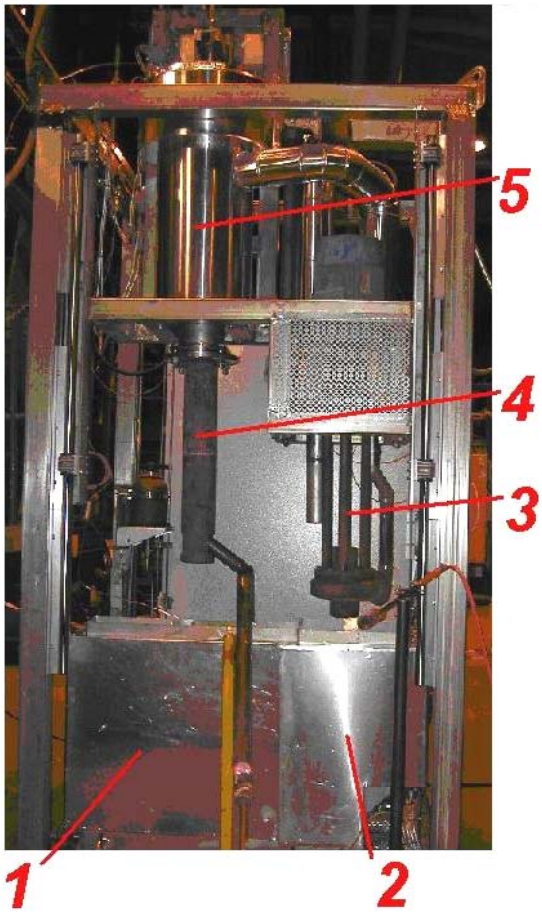

Figure 10. Physical model design; 1:Mould; 2:Pump section; 3:Centrifugal pump; 4:Casting nozzle; 5:Tundish

The process starts by melting the metal in the mould and pumping section. As the metal is molten, the upper section which consists of a tundish and a centrifugal pump is submerged into the bath, figure 11. The pump is started by a process operator as soon as the section is in position, it can be regulated at specific velocities. Molten metal will thereby be transported up to the tundish by the pump and continuously delivered into the mould through a submerged entry nozzle and thereby simulate the sequence of continuous casting. There is an inclination in the bottom of the mould that passes the alloy forward to the pump through a hole in the wall between the sections and the cycle can thereby be repeated. Heating elements in the bottom of the mould prevent the metal from being solidified.

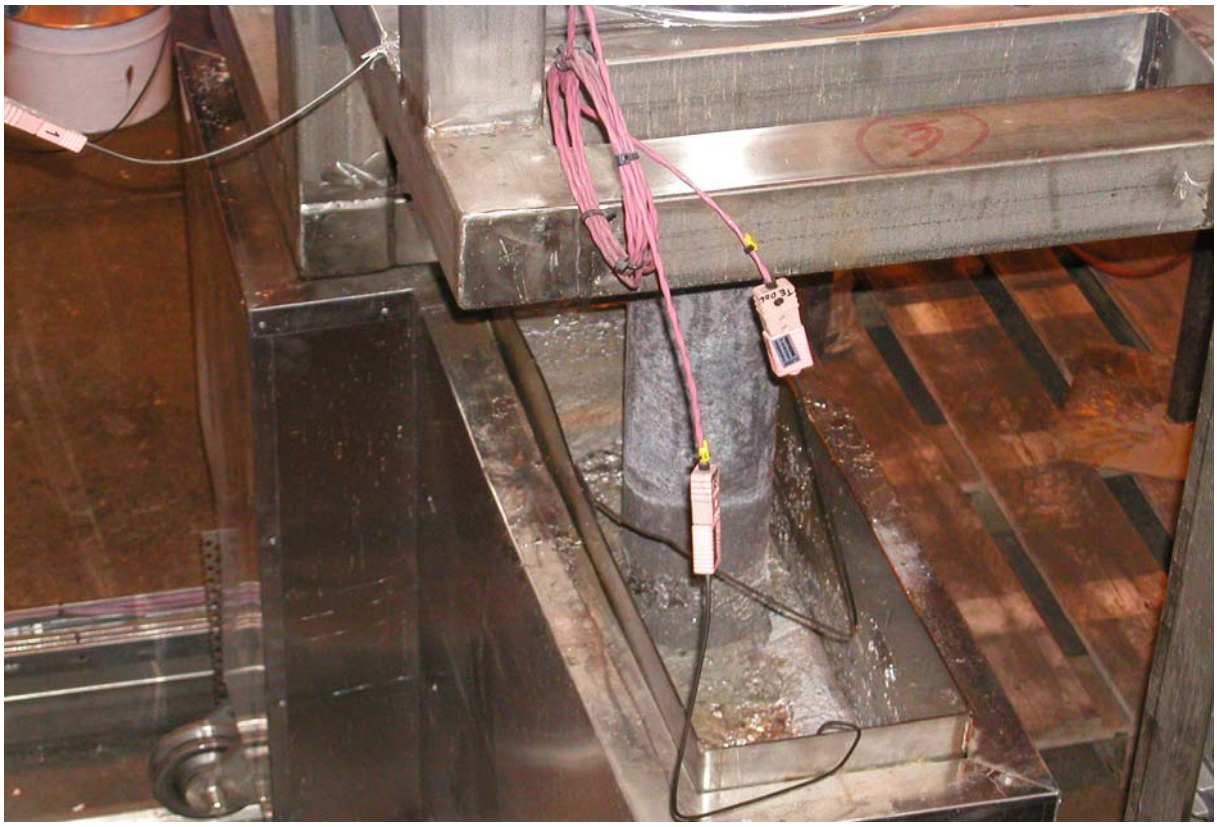

Figure 11. Physical model at simulation. The nozzle is submerged into the mould.

Figure 11 also reveals formation of dross that appears in the tundish. As the simulation starts, the tundish is empty. The alloy will thereby be strongly exposed to air and an oxidation will be unavoidable. The formation of oxide dross drastically decreases as soon as the process stabilises.

3.4.3.1 Pumping section

The pumping section is connected to the mould and thereby continuously fed by liquid alloy. A centrifugal pump delivers metal to the tundish at different casting rates. There are four heating elements in the vessel to keep the alloy molten, two in the bottom which are consistently into the mould and two short elements further up in the vessel.

The flow of metal in the physical model is driven by the velocity of the pump. The process operator runs the pump at different speeds through a regulating system, developed at MEFOS, on a computer.

3.4.3.2 Tundish

The centrifugal pump delivers molten alloy from the pumping section up to the tundish. The inlet is placed at the middle of the tundish. This design prevents the alloy from being oxidised during the simulation.

The tundish has a vessel as protection if it would be over filled. This vessel is connected to the pumping section so the alloy can be recovered if an accident should occur. The level in the tundish is registered by a laser and viewed on the process computer.

The tundish has a height of 0.90 and a diameter of 0.25 metres respectively. The flow of alloy into the mould is regulated by a stopper rod. This is in turn regulated by a hydraulic system through a process computer. It is possible to regulate the stopper upward and downward, from zero to 65 millimetres. The radius of the stoppers head is 0.06 metres.

As the alloy leaves the tundish, it enters the submerged entry nozzle. The nozzle has a diameter of the bore of 0.07 metres, radius of seat of 0.05 metres and a length of 0.970 metres. The stopper and the casting nozzle can be studied in figure 5.

3.4.3.3 Mould

The mould has the dimensions 0.22*x*0.80 metres. The length of the mould is 0.9m. The dimensions of the mould in the physical model are a commonly used geometry in continuous casting.

The mould has two elements in the bottom that keeps the temperature of the metal. These elements are elongated through a hole in the wall to the pumping section. There is an inclination in the bottom so the alloy can flow through the mould to the pumping section, so continuous casting can be simulated.

3.4.3.4 Start of the model

This report is concentrated on the experiments with molten metal, but when the model was brought into use, experiments with water were done. This was both to ensure the security of the model, for instance leakage but also to decide different flow of water at specific velocities of the pump.

When the alloy was inserted to the system, the elements in the mould and pumping section had to be protected against injuries. Bars were therefore added to the vessels through a special feeder system. The feeder was heated with a burner and the alloy was consequently melted. As soon as the elements were covered with metal, the two sections were filled with bars.

A warming procedure started when the sections were completely filled with bars and as the alloy subsided, more bars were added. The procedure was continued until the sections were filled with a homogenous mass. This procedure took several hours due to gaps of air between the bars. It should also be noticed that the effect of the elements was not driven to its maximum effect the firs times.

Before the experiments, heating of pump and stopper rod have to be made to avoid metal to stick on a cold pump and also avoiding the stopper to expand. This heating was done with burners. When a temperature of about 200 degrees was reached, the top section was inserted to the bath section.

3.5 Compact laser vibrometer

A compact laser vibrometer, also called CLV, is used for non-contact measurement of surface vibration velocity. The CLV is made up of the controller and the sensor head. The light source of the CLV is a helium neon laser and has a wave length that refers to 633 nm.

A fluid that passes through a pipe causes vibrations related to the velocity of the fluid. The compact laser vibrometer is a previously used technique that measures the vibrations at the surface of the casting nozzle. By measuring the vibrations of the casting nozzle, the flow through the nozzle may be described.

Earlier studies were done in a water model with gas injection [22]. It was possible to observe a difference in the signal intensity and frequency, depending on the flow pattern inside the nozzle. Stronger mean signal intensity could be seen for annular flow, but also the maximum peak that was located at higher frequencies than for bubbly flow.

3.5.1 Measurement principle

A CLV measures vibration velocities on the basis of laser interferometry. The beam of the laser is pointed at the vibrating object, in this case a submerged entry nozzle, and scattered back from it. The object beam is thereby subjected to a small frequency shift which is described as the Doppler frequency, f_D. The Doppler frequency is a function of the velocity component v in the direction of the object beam according to;

$$f_D = 2 * \frac{|v|}{\lambda} \quad \textbf{(8)}$$

f_D= Doppler frequency
v= velocity component in the direction of the object beam
λ= wavelength of the laser,

If the object beam is superimposed with an internal reference beam, beating is generated. Beating means that the intensity of the resulting beam fluctuates periodically.
The beat frequency is equal to the Doppler frequency. It however is dependent of the direction of the velocity and it is thus ambiguous.

The direction is determined by introducing an additional fixed frequency shift, f_B in the interferometer to which the Doppler frequency adds to generate an unambiguous signal form. Thus for the resulting frequency shift at the detector f_{mod} we have

$$f_{\mathrm{mod}} = f_B + 2 * \frac{v}{\lambda} \qquad \textbf{(9)}$$

f_{mod}= *Resulting frequency shift at the detector*
f_B= *Fixed frequency shift*

The resulting signal is transmitted to the controller and decoded. A voltage is generated and this is proportional to the instantaneous velocity of the vibrating object.

4 Measurements

A simulation based on a single phase flow is considered in the investigation. The stopper rod was therefore plugged during the experiments. The goal with the experiment was to examine the responsiveness of the compact laser vibrometer at specified volumetric flows.

4.1 Experiments

The flow in the physical model is determined by the velocity of the pump. To be able to perform the measurements, a calibration of the pumps velocity had to be done. It is important to know the flow at a specific pumping velocity to be able to correlate this flow with the signals from the sensors.

The immersion depth in the mould and the height in the tundish were kept constant to make sure of a stable flow.

4.1.1 Determination of volumetric flow

As mentioned earlier there is no commercially used system to detect the velocity of steel. The flow of metal in the model was determined indirectly by using the filling time of the tundish and the volume of the same. Experiments were done to be able to specify the flow of molten alloy as a function of pumping velocity.

The flow can be determined theoretically if the open area between stopper and seat of the casting nozzle is calculated as a function of stopper lift, appendix A. Pressure has to be known in some key location and these can according to Bolger [6] be calculated based on Bernoulli's equation.

The performance of the experiments was as follows; the stopper rod was open when pumping at a specific speed of the pump. As the stopper closed, the time it took to fill the tundish was registered both by a laser, positioned in the arm to the stopper and by hand. These experiments were repeated for several velocities and flow as a function of pumping velocity could thereby be determined. Due to delays of the laser, it was decided that times measured by hand should be considered when the flow was calculated.

4.1.1.1 Pre-calculations

The volume of the tundish is 33.44 dm^3 if the stopper rod is approximated with a cylinder. Times to fill the tundish were measured for different velocities of the pump and the volumetric flow of steel in the tundish as a function of the velocity of the pump could be determined. The result is illustrated in figure 12.

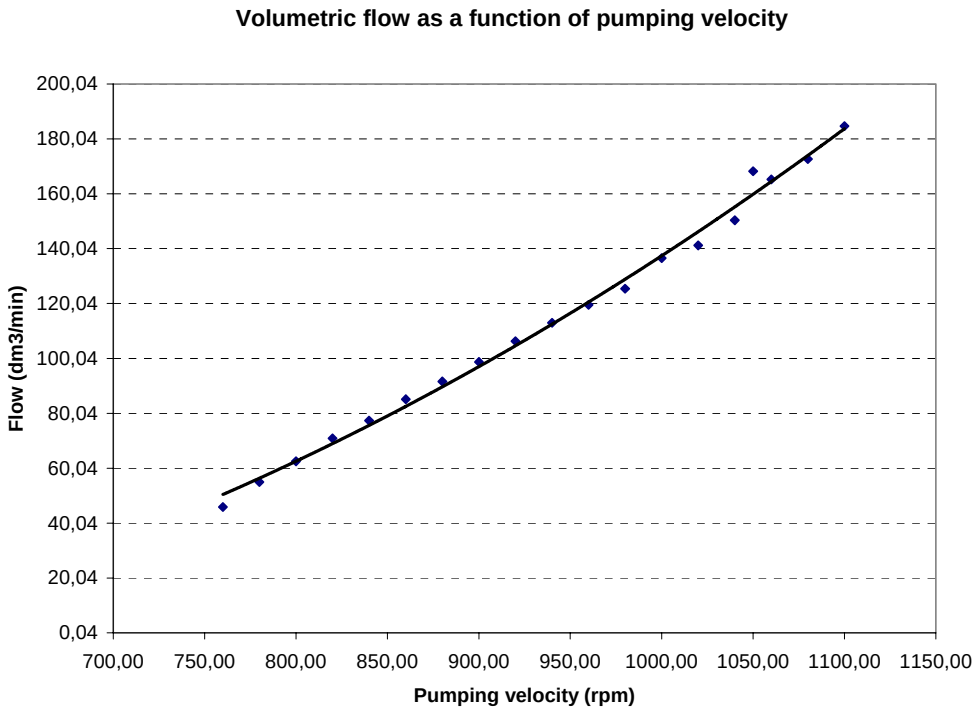

Figure 12. Calculated volumetric flow in tundish as a function of pumping velocity

The calculated flow in tundish can be considered as a polynomial function of pumping velocity;

$$Q = 4{,}93 * 10^{-6} x^2 - 2{,}64 * 10^{-3} x \qquad \textbf{(10)}$$

$Q =$ Calculated flow of alloy in tundish (dm^3/s)
$x =$ Pumping velocity (rpm)

The flow in the model is constant and there is a constant cross section of the submerged entry nozzle and the mould in the physical model. The velocities in the nozzle and the mould can thereby also be calculated.

The cross sectional area of the casting nozzle and the mould is 0.0038 and 0.16 m^2 respectively. The volumetric flow in tundish is divided with each of the two cross sections and the velocity is calculated. The calculation is possible when accumulation not occurs in the system. The results are shown in figure 13 and 14.

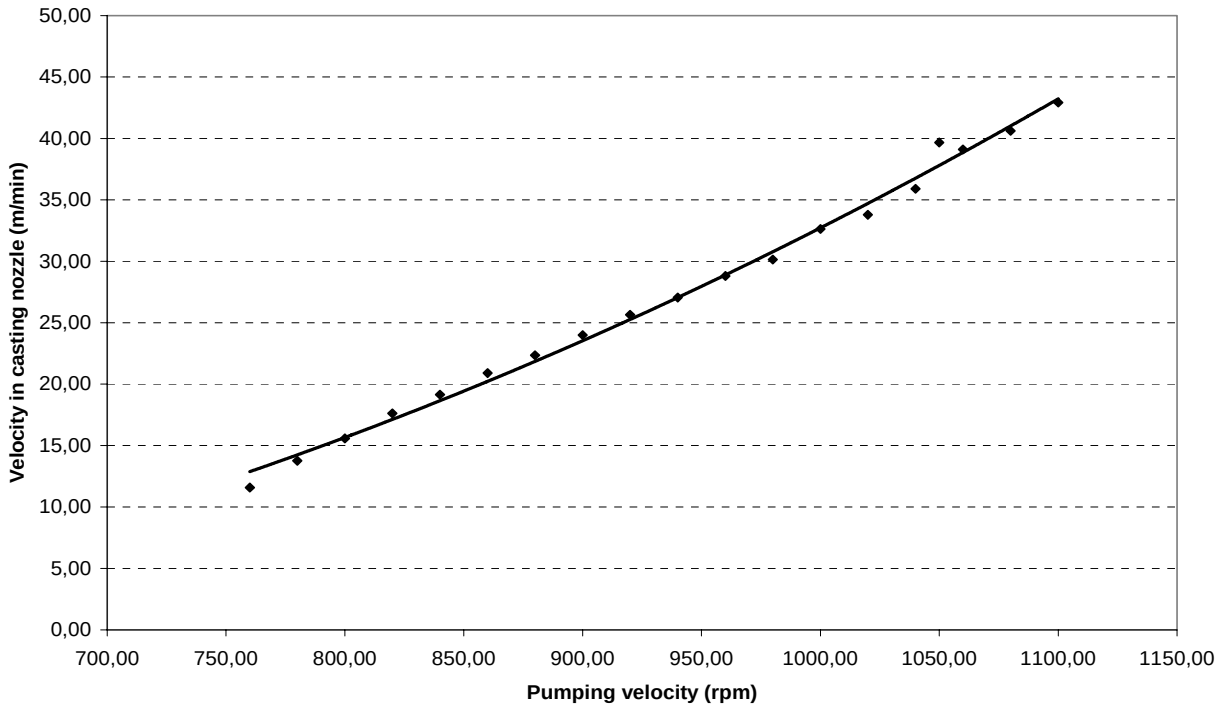

Figure 13. Calculated velocity in the submerged entry nozzle as a function of pumping velocity

If the velocity in the casting nozzle is calculated as a function of the velocity of the pumping velocity, it can be expressed by equation (11):

$$s = 6{,}57 * 10^{-5} x^2 - 3{,}30 * 10^{-2} \quad \textbf{(11)}$$

s = Calculated velocity of the alloy in the submerged entry nozzle (m/min)
x= Pumping velocity (rpm)

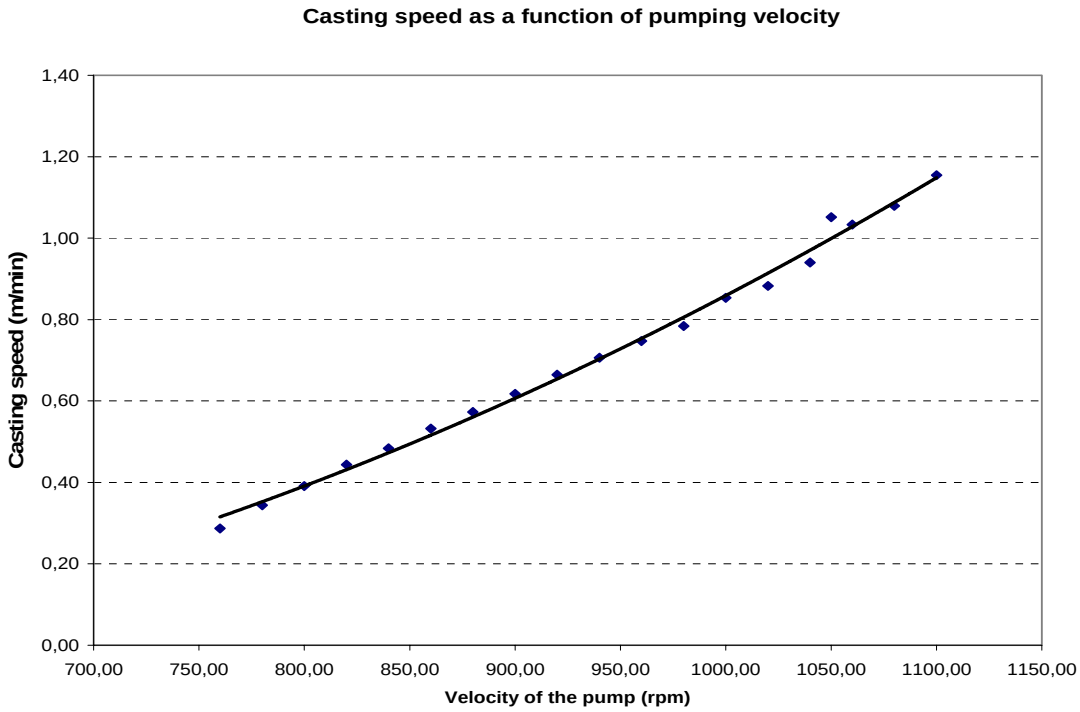

Figure 14. Calculated casting speed as a function of pumping velocity

Calculated casting speed can be expressed as a polynomial function of the pumps velocity

$$c = 1{,}85 * 10^{-6} x^2 - 0{,}99 * 10^{-3} x \qquad \textbf{(12)}$$

c = Calculated casting speed (m/min)
x = Pumping velocity (rpm)

4.1.2 Design of experiments

9 specific flows according to table 1 were to be examined during the experiments.

Table 1. Alloy experiments

Experiment	Pumping velocity (rpm)	Flow (dm^3/s)	Calculated casting velocity (m/min)	Immersion depth (m)	Height in tundish(m)
1	750,00	0,79	0,30	0,30	0,86
2	800,00	1,04	0,39	0,30	0,86
3	850,00	1,31	0,49	0,30	0,86
4	900,00	1,61	0,61	0,30	0,86
5	950,00	1,94	0,73	0,30	0,86
6	1000,00	2,29	0,86	0,30	0,86
7	1020,00	2,43	0,91	0,30	0,86
8	1050,00	2,66	1,00	0,30	0,86
9	1100,00	3,06	1,15	0,30	0,86

Data were collected using logging on process computers. A computer was connected to each of the sensors and also to the regulating system of the physical model. Data were synchronized using time and the velocity of the pump.

It has been discussed earlier that it is important to have a laminar flow in the mould. Calculation of the Reynolds number is done in appendix B, and it can from table B1 be seen that it is difficult to have a laminar flow in the physical model. The alloy has a comparable density with steel and a lower viscosity. This implies a turbulent flow in the model at the applied volumetric flow. A comparison with steel at the same pumping velocities are also calculated in appendix B, table B2. Steel has a higher viscosity and might have laminar flow in the mould at the flow conditions used at this simulation.

There were some discussions in chapter 4.4.1 about physical modelling and that Reynolds number was important in laminar flow modelling and became less important in turbulent flow modelling [16]. This should imply that the Froude number is valid in this model.

4.2 Pre-processing of data

The height of metal in the tundish were kept constant at 0.86 m and the immersion depth in the mould were also constant at 0.3 m during the experiments., so the flow can be considered as steady state.

The signal from the compact laser vibrometer was investigated. The signal intensity was logged over a frequency spectrum, reaching from zero to 120 Hz. A correlation of data at the pumping velocities 700, 750 and 1100 rpm could not be made. Data from 820 and 1090 rpm was considered instead and a total of eight flows were investigated.

To be able to detect at which frequencies the clearest intensities could be seen, the mean signal intensity was calculated as a function of frequency at the different flows. The clearest signals refer to the frequency span of 0-30 Hz and this spectrum is thereby considered in further this report.

As the engine of the pump creates vibrations measurements were also conducted on the engine during the measurements hereby facilitating the possibility to compensate for this background noise in further analysis.

Figure 15 shows how the signal from the laser compact vibrometer was studied. If the measurements that was done on the casting nozzle is considered as $f(x)+g(x)$, where the signal from the flow is $f(x)$ and the background noise is $g(x)$, a corrected signal from the flow $f(x)$ can be studied by subtracting the background noise from the measurements made on the casting nozzle.

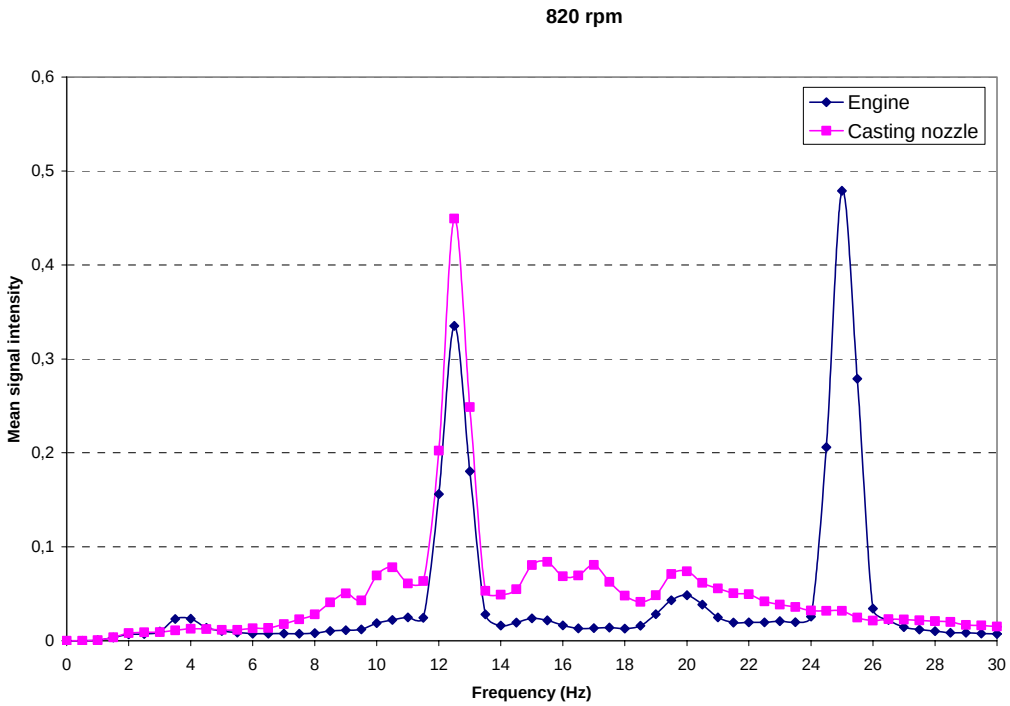

Figure 15. The signal from the compact laser vibrometer shows here the mean signal intensity over the frequency spectrum 0-30 Hz at a pumping velocity of 820 rpm

5 Results

The corrected signal is presented in the results. Measurements made on the casting nozzle and on the engine of the pump can be studied in appendix *C*, figure *C1-C8*.

5.1 Responsiveness of the compact laser vibrometer

The background noise of the engine is excluded and the corrected signal is considered in figure 16 to figure 23. The mean signal intensity can be studied on the *y*-axis and the frequency spectrum 0-30 Hz on the *x*-axis respectively. Each diagram refers to a specific velocity of the pump and thereby a specific flow in the model.

5.1.1 Peak frequency

A pumping velocity of 820 rpm is the lowest velocity that was possible to correlate to the vibration measurements. As the pump runs on a velocity of 820 rpm, the flow in the model is 1.15 dm^3/s.

If the response of the signal is studied, it can be seen that the largest peak is visual around 12.5 Hz. Smaller peaks can also be seen at frequencies of 9, 10.5, 15, 17, 19 and 21 Hz. There seems to be areas where the background noise totally depresses the signal from the flow. These areas can be seen around 3-5 Hz and 24-26.5 Hz in figure 16.

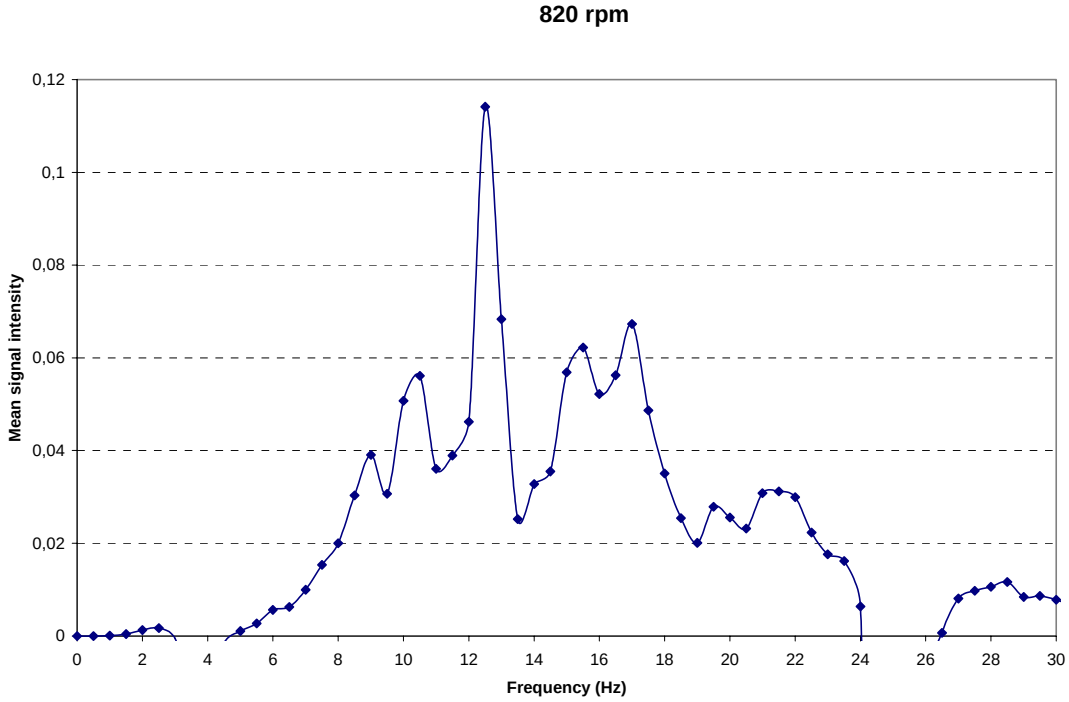

Figure 16. Mean signal intensity as a function of frequency in a spectrum reaching from zero to 30 Hz at a pumping velocity of 820 rpm.

Figure 17 shows the response of the signal measured on a pumping velocity of 850 rpm. A pumping velocity of 850 rpm corresponds to a flow of 1.31 dm^3/s. The highest peak has moved slightly to the right, compared with the measurements made on a pumping velocity of 820 rpm. The highest peak is located at 13.5 Hz.

Figure 17 shows smaller peaks at the frequencies 9, 10.5, 15, 17, 19 and 21 Hz. These peaks could also be seen in figure 16

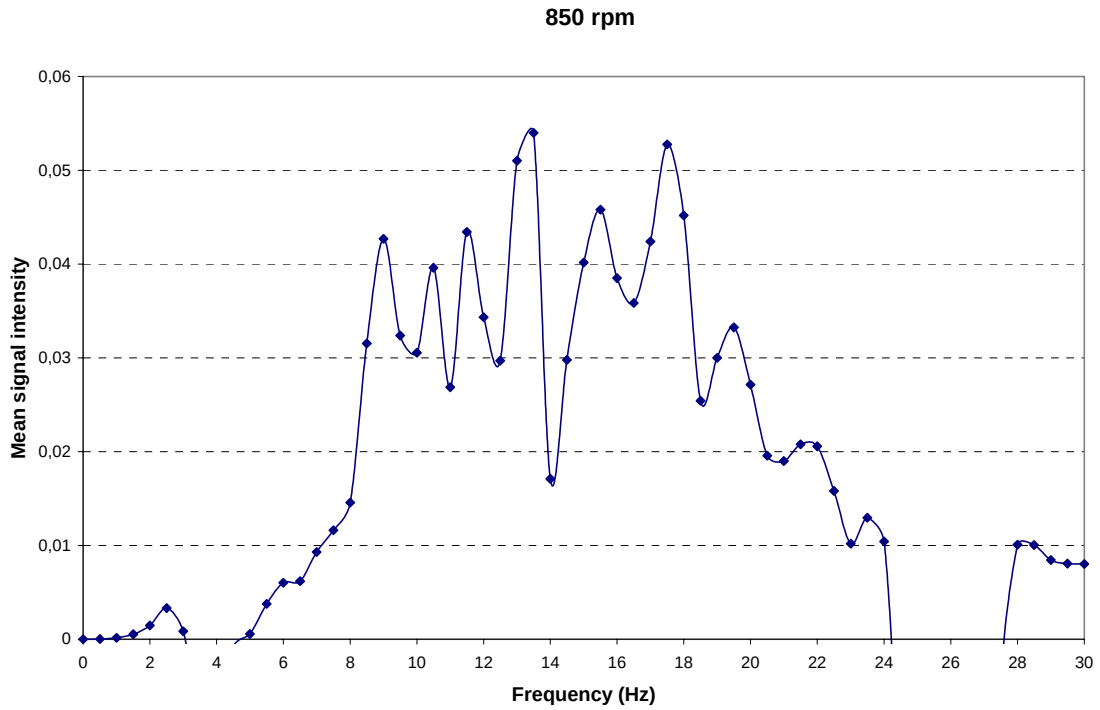

Figure 17. Mean signal intensity as a function of frequency in a spectrum reaching from zero to 30 Hz at a pumping velocity of 850 rpm.

Figure 18 shows the difference in signals measured with the compact laser vibrometer on the casting nozzle and the engine of the pump. The pumping velocity was 900 rpm and this velocity contributes to a volumetric flow of 1.61 dm3/s in the physical model.

The largest peak is found at 10.5 Hz. If we compare this signal, with the earlier that was studied at 820 and 850 rpm respectively, the largest peak can be suspected to be found around 14 Hz. Figure 18 shows that the signal from the flow is suppressed by the background noise around this frequency in agreement with figure *C3* in appendix *C*.

Figure 18 also shows that smaller peaks are visual around the same frequencies as discussed earlier. The amplitudes of these smaller peaks are therefore to be studied later in the report.

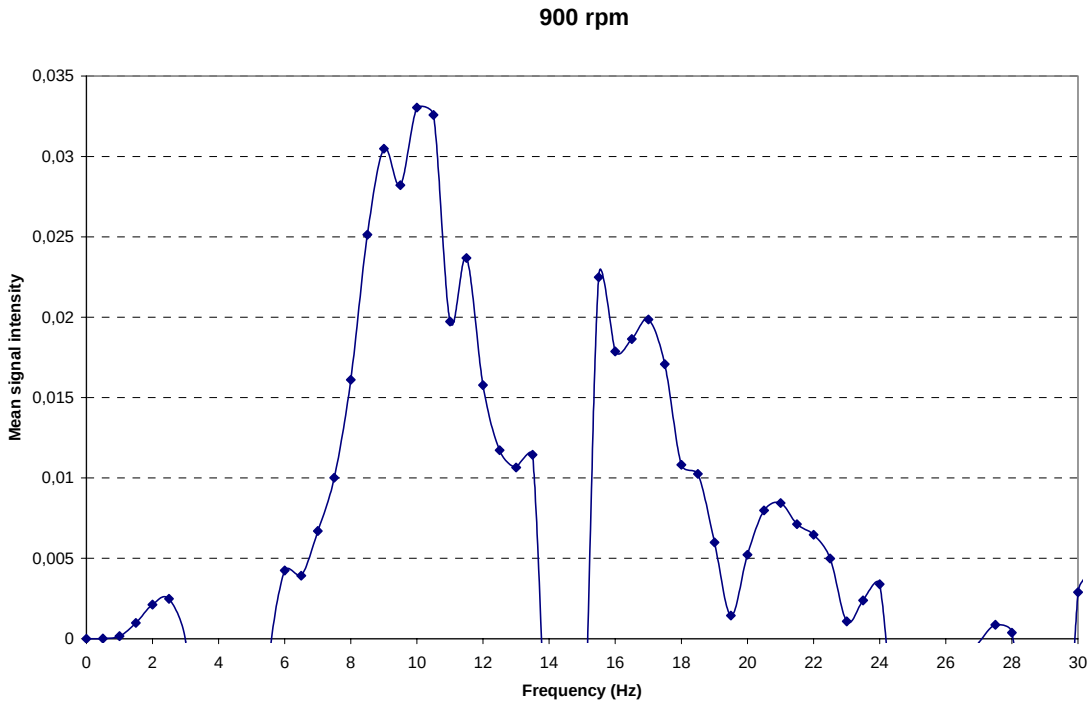

Figure 18. Mean signal intensity as a function of frequency in a spectrum reaching from zero to 30 Hz at a pumping velocity of 900 rpm.

The volumetric flow in the physical model is 1.94 dm^3/s when the pump is running on a velocity of 950 rpm. The maximum peak is located at a frequency of 14.5 Hz, which can be seen in figure 19, but large peaks are also visual at 7 and 21 Hz.

Figure 19 shows also that there are some activities at the frequencies for the smaller peaks, mentioned before.

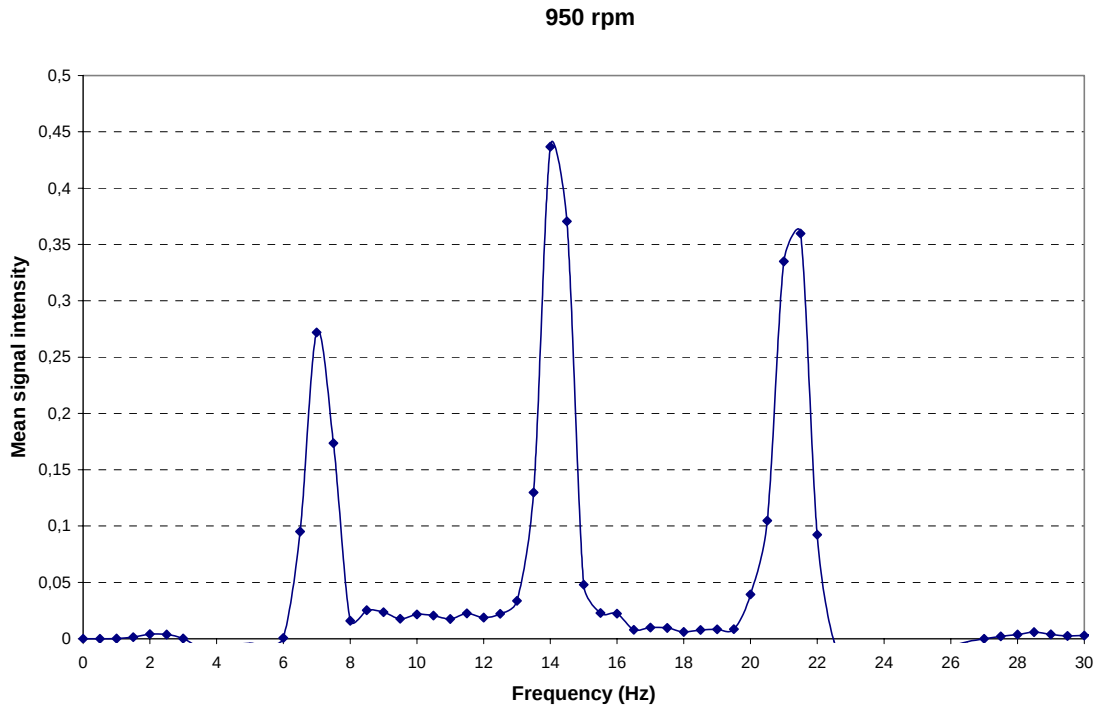

Figure 19. Mean signal intensity as a function of frequency in a spectrum reaching from zero to 30 Hz at a pumping velocity of 950 rpm.

Figure 20 shows the difference between the measurements made on the casting nozzle and the engine of the pump when the pump is running on a velocity of 1000 rpm. The volumetric flow in the physical model is 2.29 dm^3/s. The clearest peak, and thereby the highest response of the measurements, is located around 17 Hz. The smaller peaks are still visual.

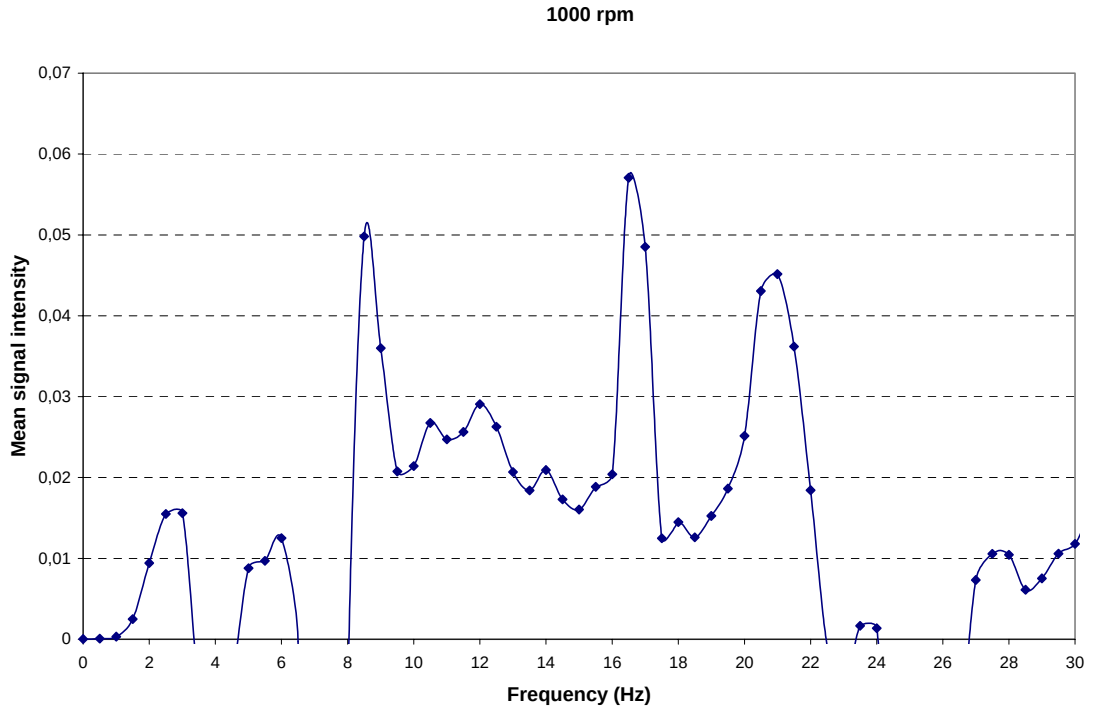

Figure 20. Mean signal intensity as a function of frequency in a spectrum reaching from zero to 30 Hz at a pumping velocity of 1000 rpm.

As the velocity of the pump reaches 1020 rpm, the velocity in the mould of the physical model is 0.9 m/min. 0.9 m/min is a normal casting speed at continuous slab casters. A pumping velocity of 1020 rpm refers to a flow in the physical model of 2.46 dm^3/s

Figure 21 shows that the largest peak is located at a frequency of 17.5 Hz and that the smaller peaks can be found at the expected frequencies.

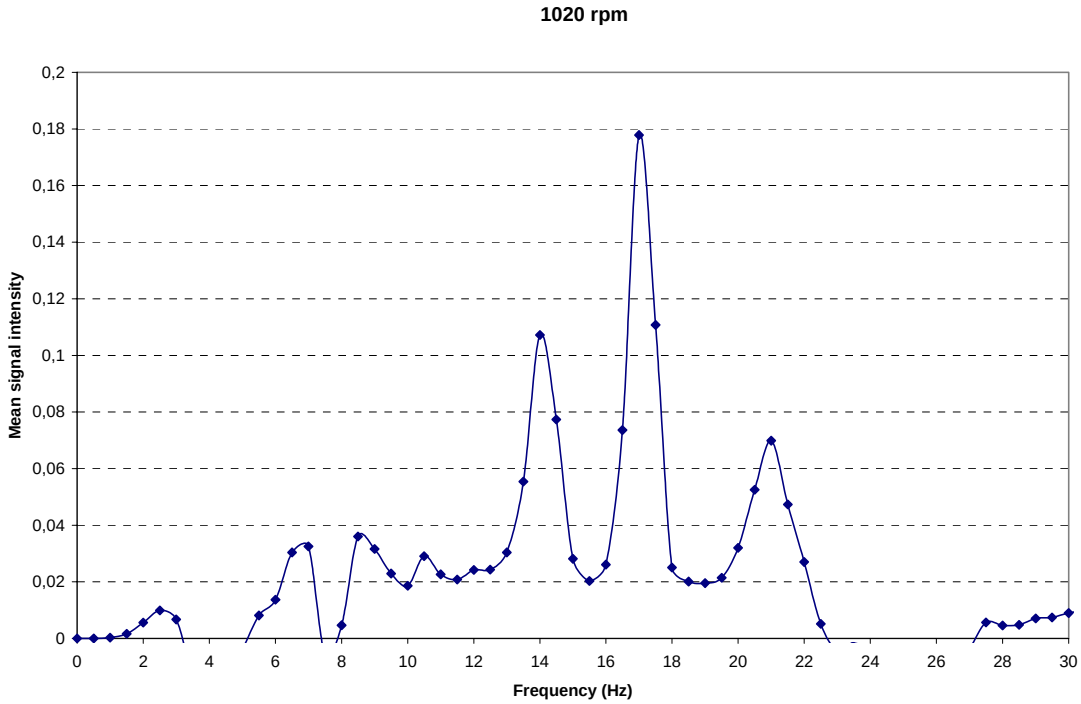

Figure 21. Mean signal intensity as a function of frequency in a spectrum reaching from zero to 30 Hz at a pumping velocity of 1020 rpm.

The volumetric flow in the physical model is 2.66 dm^3/s when the pump is working at a velocity of 1050 rpm. Figure 22 shows the difference between the measurements made with the compact laser vibrometer on the casting nozzle and the engine of the pump.

The highest peak at a pumping velocity of 1050 rpm can be seen at a frequency of 13 Hz. This is surprising, due to the trend of increasing frequency at higher flows. What happens here seems to be the same that occurred at a pumping velocity of 900 rpm. The largest peak of the signal measured on the casting nozzle is suppressed by a large background noise, created by the engine. The largest peak is thereby located at another frequency than expected. A comparison can be done with figure *C7* in appendix *C*.

Smaller peaks are still visual at expected frequencies, i.e. at frequencies around 9, 10, 19 and 21 Hz.

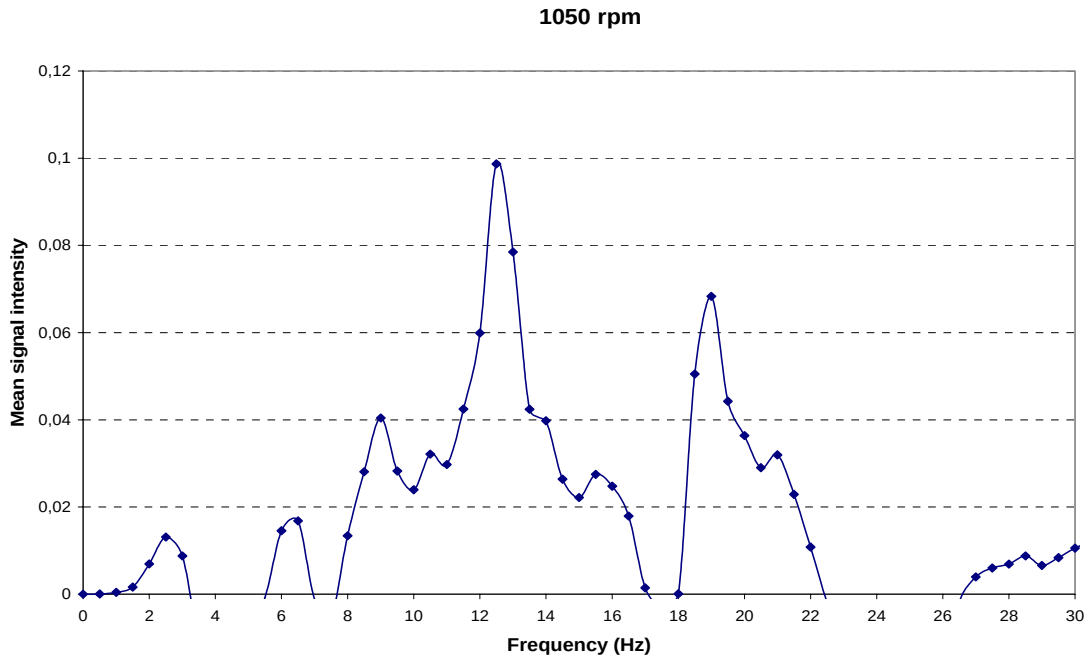

Figure 22. Mean signal intensity as a function of frequency in a spectrum reaching from zero to 30 Hz at a pumping velocity of 1050 rpm.

A pumping velocity of 1090 rpm refers to a volumetric flow of 2.98 dm^3/s in the physical model. This is the measurement done at the highest velocity of the pump and thus the highest volumetric flow in these experiments. The highest peak is located at 18 Hz in the frequency spectrum, figure 23.

The smaller peaks are still located at constant frequencies in the spectrum and are to be studied separately in the summation that follows.

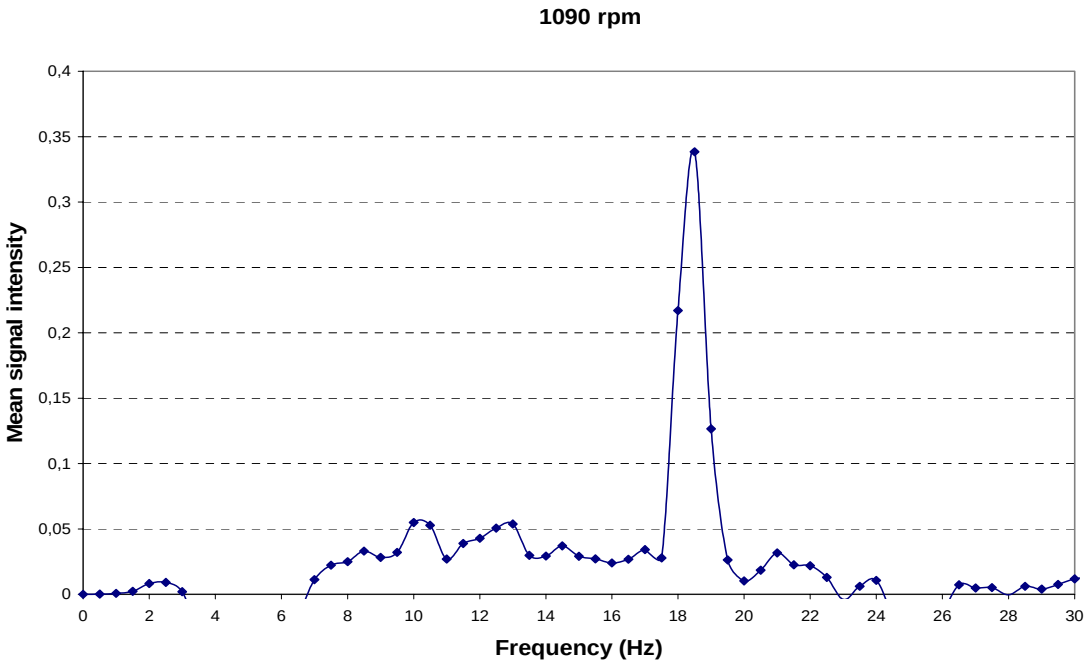

Figure 23. Mean signal intensity as a function of frequency in a spectrum reaching from zero to 30 Hz at a pumping velocity of 1090 rpm

5.1.2 Peak frequency, amplitude and volumetric flow

The peak with highest mean signal intensity and thereby highest amplitude for the measurements made on the casting nozzle is located at the same frequency as a large peak measured on the engine, see figures *C1-C8* in appendix *C*. The frequency of this peak is shown as a function of flow in the model in figure 24. A trend of higher frequency at higher flows can be studied for the signal where no background noise is excluded.

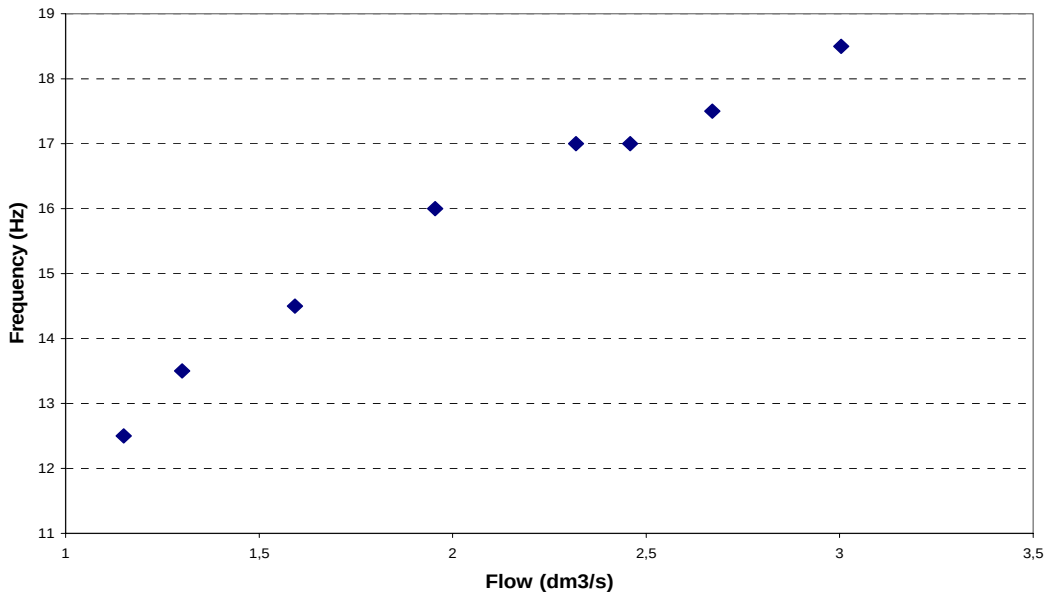

Figure 24. Frequency as a function of flow for the largest peak of the measurements made on the casting nozzle for all flows measured

The amplitudes of the peak in figure 24 can also be studied as a function of flow. The amplitudes of this peak are studied in figure 25 for both the measurements made on the engine and the measurements made on the casting nozzle. A parabolic pattern seems to appear and a minimum of the amplitude is visual just below a flow of 2 dm^3/s.

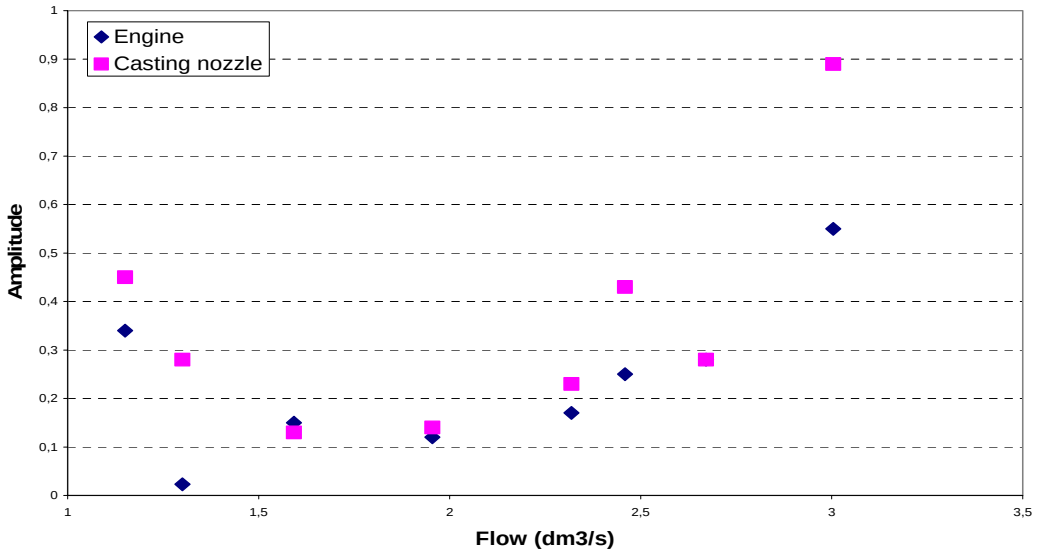

Figure 25. Amplitude as a function of flow for the highest peak measured on the casting nozzle. The signal from the engine shows a clear peak at the same frequencies, which is also shown in the diagram

If we exclude the background noise from the engine and consider the amplitude of the highest peak of the corrected signal, figure 16-23, it can be seen that the highest peak refers to the same peak as studied in figure 24, except for two flows where the signal from the engine seems to depress the signal from the flow. This was earlier discussed at measurements made on a pumping velocity of 900 and 1050 rpm.

The amplitudes of the highest peak of the corrected signal are considered in figure 26. The same type of parabolic pattern seems to occur here as in figure 25, with a minimum below 2 dm^3/s if the amplitude of the peak at a flow 1.95 dm^3/s is considered as a not representative value.

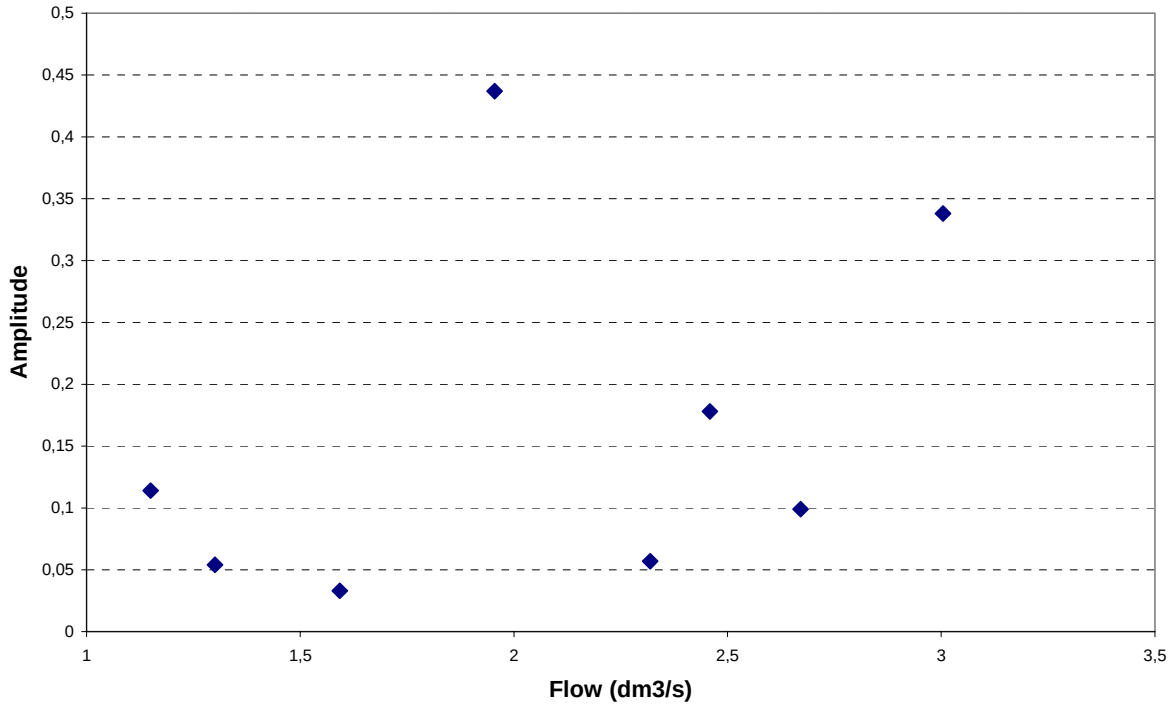

Figure 26. Amplitudes as a function of flow of the highest peak of the corrected signal

5.1.3 Amplitudes at constant frequencies

The main discussion has been about the largest peak in the spectrum, but smaller peaks have also been visual. The discussion of smaller peaks refers to the peaks that seem to be located at rather constant frequencies of 9, 10.5, 15, 17, 19 and 21 Hz.

Figure 27, 28 and 29 shows the amplitudes of the peaks located around 9 and 10.5 Hz, 15 and 17 Hz, 19 and 21 Hz respectively.

A similar pattern as the amplitudes of the highest peak can be seen. A minimum in amplitude seem to occur around a pumping velocity of 950 rpm and thereby a flow of 1.95 dm^3/s. Some type of disturbance can be seen at higher flows for the peaks located at 15, 17, 19 and 21 Hz. This is most lightly disturbances caused by the largest peaks that move to higher frequencies at higher flows.

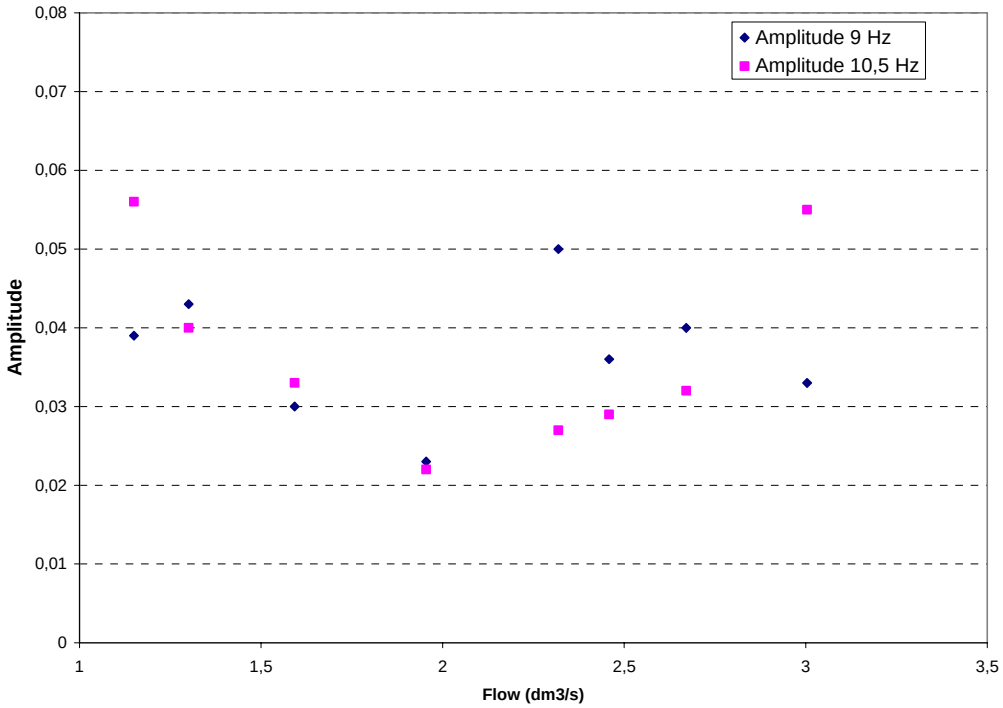

Figure 27. Amplitudes for the peaks located at 9 and 10.5 Hz

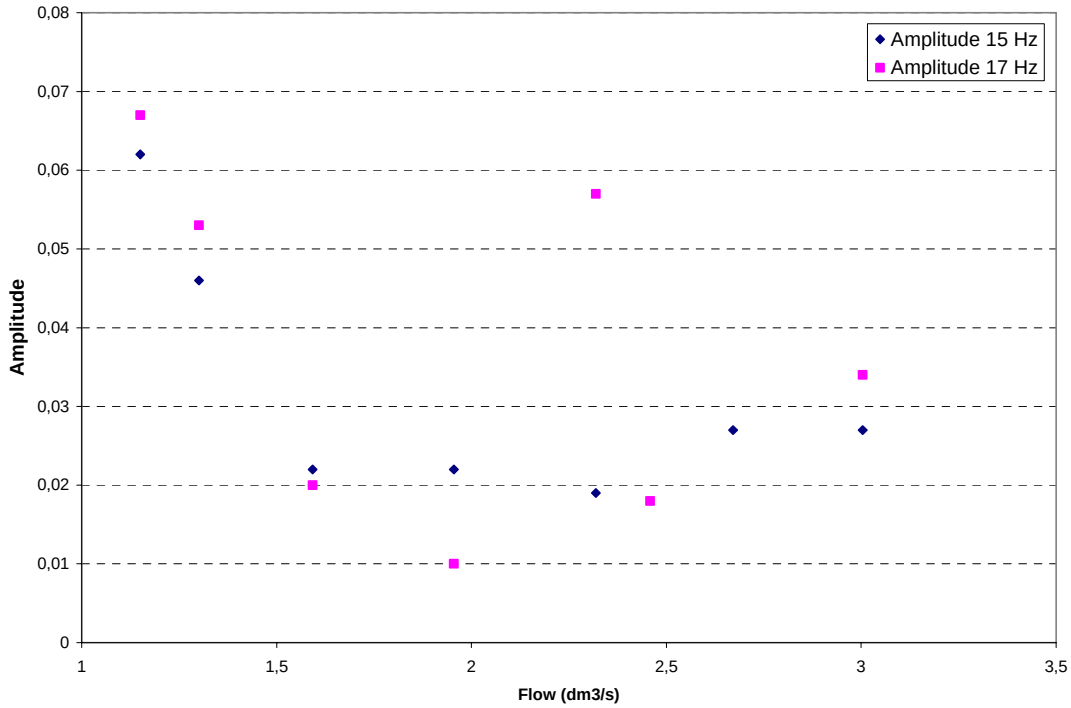

Figure 28. Amplitudes for the peaks located at 15 and 17 Hz

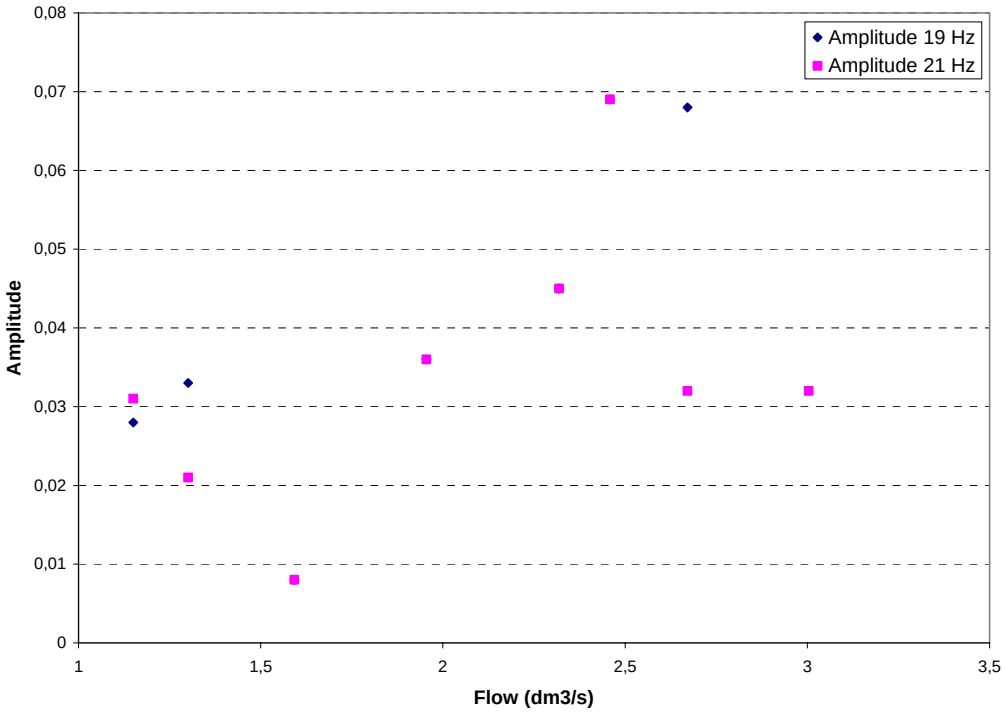

Figure 29. Amplitudes for the peaks located at 19 and 21 Hz

5.1.4 Amplitudes and stopper position

A test was done to examine the consistency of the flow during simulation. The velocity of the pump was kept constant during 1.5 hours.

The stopper is the main key to a constant flow in the model. If deviations occur at simulation in the model, a constant level in the tundish and mould can be held by regulating the stopper upwards and downwards.

Figure 30 shows the process log measured of the stoppers position as a function of the pumps velocity. The variation in stopper position is within 0.5 mm.

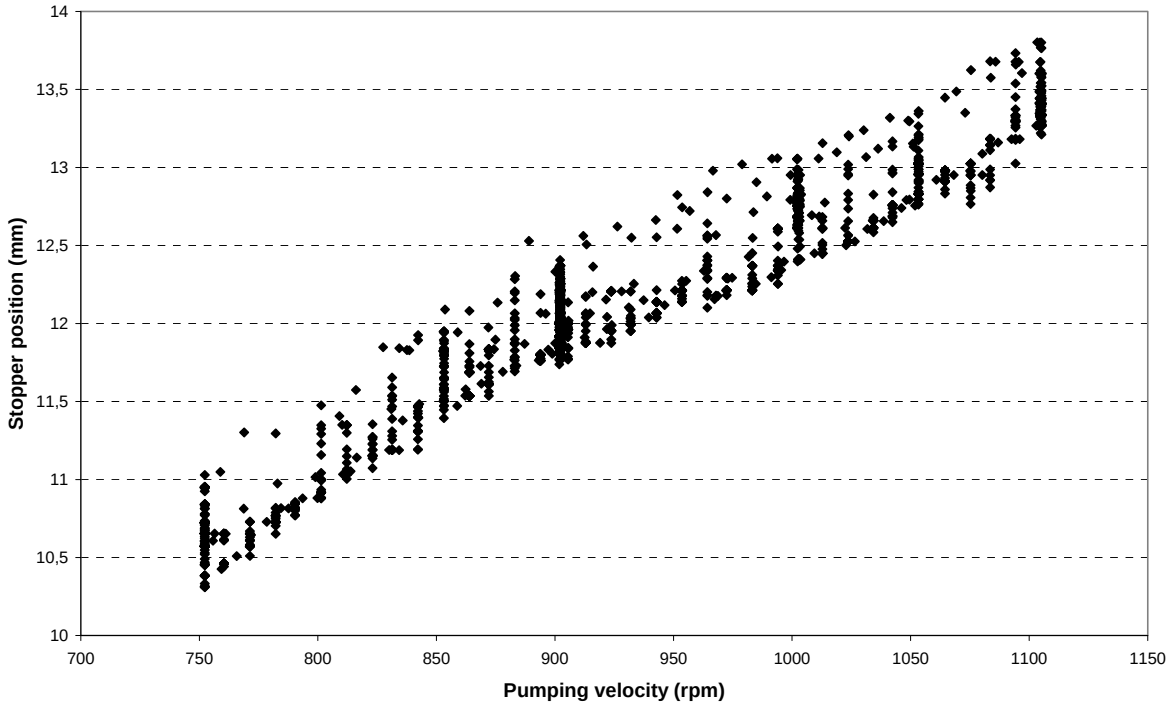

Figure 30. Stoppers position as a function of the pumps velocity

Due to earlier calculations, the flow in the model is known at specific pumping velocities. Figure 31 shows the stoppers position as a function of volumetric flow in the model. Figure 31 shows a smooth inclination up to 900 rpm and a volumetric flow of 1.6 dm^3/s. After these values, a rougher inclination can be seen.

Figure 18 shows that the peak of the flow at the expected frequency is depressed by the background noise, i.e. the engine in these measurements. The engine is running at 900 rpm at this flow. Figure 27 shows a clear decrease of the amplitude at a pumping velocity of 950 rpm.

It is possible that a disturbance of the engine occurs after a pumping velocity of 900 rpm.

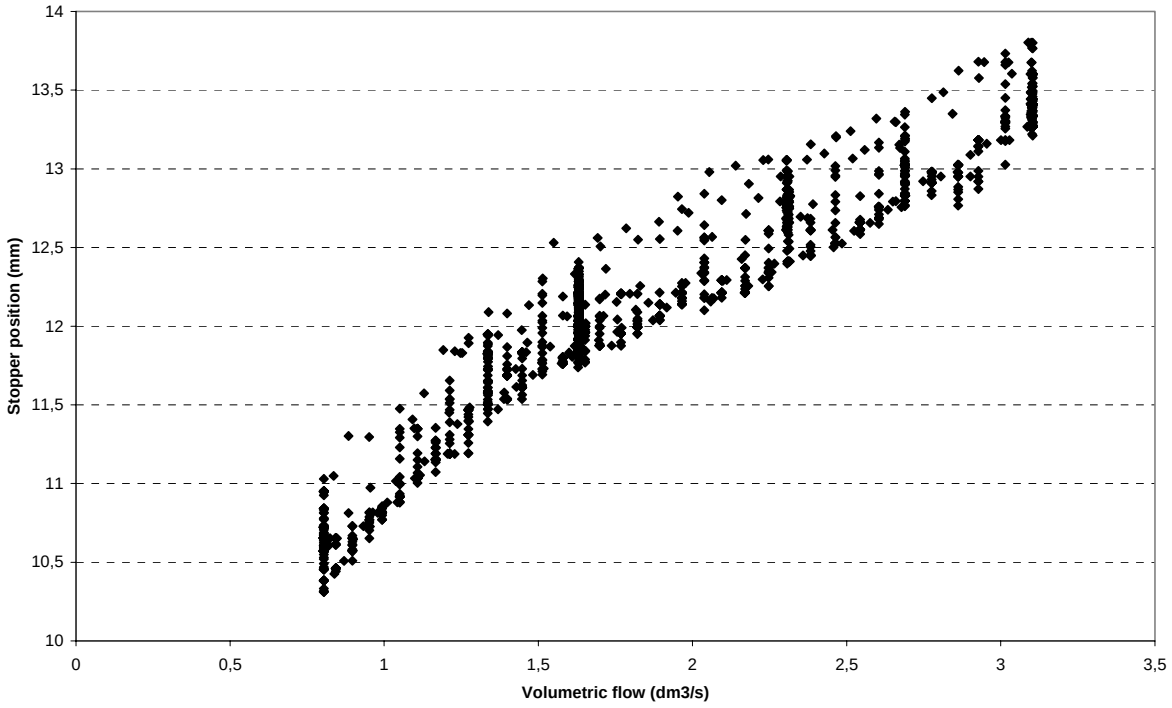

Figure 31. Flow as a function of pumping velocity

Figure 32 shows the stopper position and the amplitude as a function of volumetric flow for the peaks located around 9, 10.5, 15, 17, 19 and 21 Hz. If we study the peaks with the smaller amplitudes, located at the same frequencies in the spectrum at all measurements, it can be seen that the minimum amplitude occurs at 900 rpm and a volumetric flow of 1.6 dm^3/s.

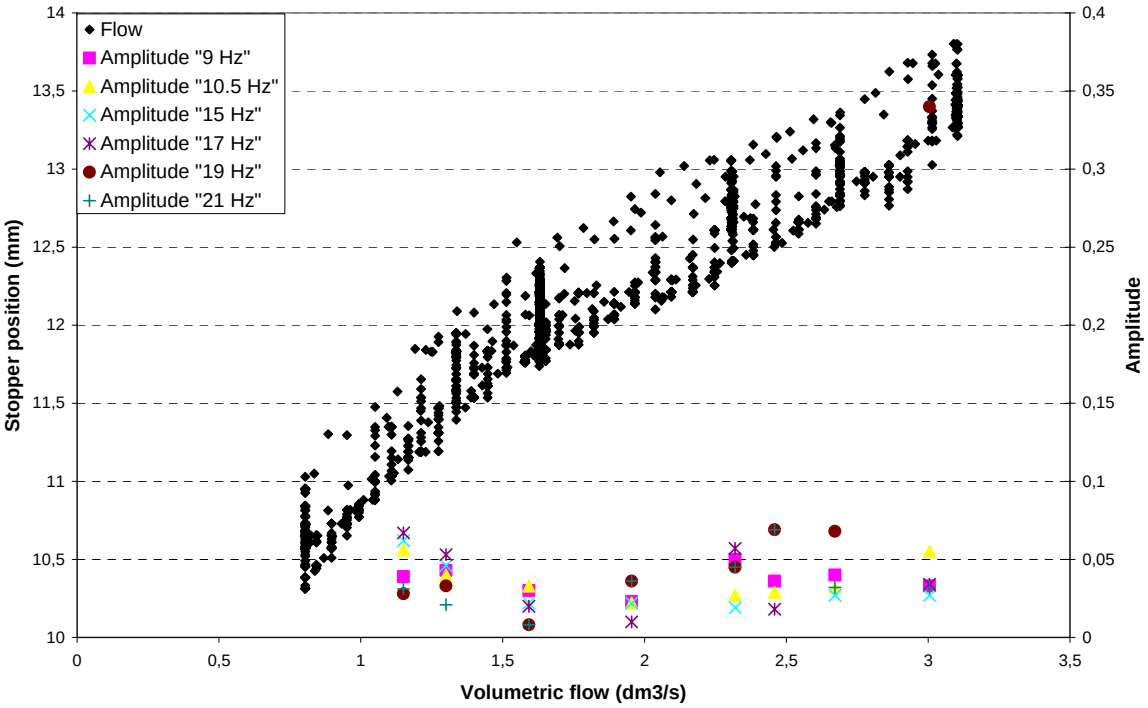

Figure 32. Stopper position and amplitude at 9, 10.5, 15, 17, 19 and 21 Hz as a function of volumetric flow in the physical model during the experiments

An interesting aspect would be to examine if the stopper can loose its ability to regulate the flow in the model. The flow is then only affected by the level in the tundish as well as the diameter of the bore of the submerge entry nozzle.

6 Conclusion and discussion

A compact laser vibrometer has been investigated in a new physical model. The model simulates continuous casting by pumping an alloy of low melting point. The alloy has except its low melting point, similar physical properties as steel. To be able to investigate the sensor at specific flows in the model, the flow of alloy was calibrated as a function of the pumps velocity.

It was found that the signal from the flow was disturbed by the engine and the signal had to be corrected. The signal showed a trend of increasing frequency at higher flow rates. The amplitudes show a general parabolic pattern. A decrease in mean signal intensity is visual until a flow of approximately 1.6 dm^3/s, where a minimum occurs.
Some deviations of the peaks located at the higher frequencies can occur at higher flows due to the movement of the largest peak to higher frequencies at higher flow rates.

The viscosity has a large influence on the Reynolds number. The viscosity of MCP 137 is an estimated value. Calculations based on the estimated viscosity points on a turbulent flow in the model. The calculated values of Reynolds number is shown in appendix B for the alloy compared to steel. Liquid iron has 3.6 times higher viscosity than the estimated value of the alloy and lies in the range of laminar flow in the mould for low velocities of the pump.
The parabolic behaviour of the amplitudes may arise from a transition from laminar to turbulent flow.

Another possibility is that the engine disturbs the signal from the compact laser vibrometer at a pumping velocity over 900 rpm, corresponding to a flow higher than 1.6 dm^3/s. A general decrease of the amplitudes can be seen up to this velocity. This seems possible because the engine has to work harder as the velocity increases and the margin between the signal from the casting nozzle and the signal from the engine decreases.

I believe that it is wise to see the results in this report as a pre-study for continued work rather than final conclusions. To be able to rely on the signal, further investigations should be made to compare with the ones discussed in this report.

7 Suggestion to continued work

The first thing to proceed with in continued work with the compact laser vibrometer should be the evaluation of a reliable signal by repeating the experiments of the single phase flows.

It is possible to generate different flow conditions in the physical model and if equivalent and reliable signals can be studied, it would be interesting to examine the intensity of the signal from two phase flows. Earlier investigations of the compact laser vibrometer in a water model have shown alterations in frequency and amplitude at the transition from bubbly to annular flow. If a two phase flow is investigated, special attention should therefore be considered around the transition between the flows in this region.

The signal strength can also be studied if other parameters are changed, such as immersion depth, length of casting nozzle and simulation of clogging.

8 References

[1] Linden, L. Detektering av igensättningar i gjutrör. Examensarbete, ISSN 1402-1617

[2] Jernkontorets informationsmaterial. Jernkontorets utbildningspaket del 4, Skänkmetallurgi och gjutning. Electronic reference at www.jernkontoret.se

[3] Fredriksson. H, Åkerlind. U. Casting processes of metals and alloys part 1 and 2 (Stockholm)

[4] Irwing, W. R. Continuous casting of steel. The institute of materials (London, 1993) ISBN 0-901716-53-7

[5] Suzuki, M. Oxidation of molten steel by the air permeated through a refractory tube. ISIJ International, vol 42 2002, no. 3, pp. 248-256

[6] Bolger, D. Stopper rod and submerged nozzle design and operation in continuous casting. 1994 Steelmaking proceedings pp 531-537

[7] Avenberg, B. Johansson, R. Optimering av nivåreglering i stränggjutningskokill. Examensarbete ISSN 0349-6023

[8] Najjar, F. M, Thomas, B. G, Hersey, D. E Numerical study of steady turbulent flow through bifurcated nozzles in continuous casting. Metallurgical and Materials transactions B: Process Metallurgy and Materials Processing Science, v 26, n 4, Aug 1995 p 749-765, ISSN 1073-5615

[9] Heaslip, L. J, Sommerville, I. D, McLean, A. Model study of fluid flow and pressure distribution during SEN injection- Potential for reactive metal additions during continuous casting. Iron and steelmaker, v 14, n 8, Aug 1987, p 49-64, ISSN 0097-8388

[10] Bai, H., Thomas, B. G. Effects of clogging, argon injection, and continuous casting conditions on flow and air aspiration in submerged entry nozzles. Metallurgical and Materials transactions B, vol 32B, August 2001, p 707-722

[11] Guy, M et al. Argon bubbling in the tundish at ACIERS D'ALLEVARD'. Florence, Italy. September 23-25, 1991

[12] Holland, F.A, Bragg, R. Fluid flow for chemical engineers (Elsevier 1995). Electronic reference at www.knovel.com

[13] Perry, R. H., Green. Perry's Chemical engineers handbook, (McGraw-Hill 1997). Electronic reference at www.knovel.com

[14] Nayvar, Mohinder, L. Piping handbook, (McGraw-Hill 2000). Electronic reference at www.knovel.com

[15] Masazumi Hirai. Estimation of viscosities of liquid alloys. ISIJ international, vol 33 1993, No 2, pp 251-258

[16] Sahai. Y, Emi. T. Criteria for water modelling of melt flow and inclusion removal in continuous casting tundishes. ISIJ International, vol 36 1996, no 9, pp 1166-1173

[17] Xiandong Ma, Anthony J. Peyton, Richard Binns, Stuart R. Higson, Electromagnetic Techniques for Imaging the Cross-Section Distribution of Molten Steel Flow in the Continuous Casting Nozzle. IEEE Sensors journal, vol 5, no 2, April 2005

[18] The valve experts. Flow of fluids through valves, fittings and pipe. Technical paper no 410 (1999 Crane CO)

[19] Lei, H, Zhu, M. Y, He, J. C. Mathematical and physical modelling of interfacial phenomena in continuous casting mould with argon injection through submerged entry nozzle. ACTA METALLURGICA SINICA (English letters) vol 13, No 5, pp 1079-1086, October 2000

[20] Coulson, J. M, Richardson, J. F. Coulson's and Richardson's Chemical Engineering, volume 1 (2003). ISBN 0-7506-4444-3

[21] Tritton, D.J. Physical fluid dynamics (1977). ISBN 0-442-30131-6

[22] Nilsson, P. Vibration measurements on a tundish pouring nozzle with a laser, water model trials. MEFOS-rapport MEF01067

[23] Sakae. T, Hirohisa. E. Theoretical and experimental studies on the resistivity of molten alloys. Transactions, Japan institute of metals. 1962 vol 3.

[24] Annual report 2001. ECSC-project. The detection and measurement of asymmetric flow in the mould and the assessment of its effect on product quality of continuously cast slabs. Mefos P4122

[25] Ellis, H. Book of data. Nuffield advanced science, 1984. ISBN 0 582 35448 X.

[26] Teng, Xin-Ying et al. Correlations between viscosity and surface tension with the structure of liquid pure iron. Material and science technology, n 4, December 2001, p 383-386. ISSN 1005-0299

9 Appendix A

9.1 Theoretical modelling of flow

Bolger [6] writes that the expected metal flows at any given stopper lift can be calculated by considering a balance of mechanical energy on a unit volume of steel flowing through the system. The Bernoulli theorem is a method of expressing the flow of fluids in a conduit by referring to mechanical energy. The total energy at any particular point, above some arbitrary horizontal datum plane, is equal to the sum of the elevation head, the pressure head and the velocity head. The pipe friction loss between two points in the system may be referred to as the head loss in metres of fluid, h_L [18].

The Bernoulli theorem is a means of expressing the application of the law of conservation of energy to the flow of fluids in a conduit. Bernoulli's equation relates the variation of speed and variation of pressure. It is valid for steady flow, where we have a fixed streamline pattern, i.e. laminar flow.

$$\frac{Q^2}{\rho * A^3} dA + \rho * g * dh + dP + \delta f = 0 \qquad \textbf{(A1)}$$

Q=Mass flow rate (kg/s)
ρ=Density of fluid (kg/m^3)
A=Cross section of conduit (m^2)
g=Acceleration due to gravity (m/s^2)
h=Height of metal column above mould meniscus)
P=Pressure (N/m^2)
f=Kinetic energy lost to friction (J/m^3)

The principal equation for continuity is valid for an incompressible fluid and involves the fact that no fluid is added or vanished into or out of the system under consideration.

$$A_1 v_1 = A_2 v_2 \qquad \textbf{(A2)}$$

A=Area (m^2)
v=velocity (m/s)
1 and 2 refers to point one and two respectively

The flow between tundish and mould is restricted by a stopper rod which is hydraulically operated through a computer by a process operator. The opening between stopper and seat of the submerged entry nozzle decides the amount of metal that should pass the valve per unit time. Bolger [6] and Avenberg/ Johansson [7] both describe this opening geometrically.

9.1.1 Open area between stopper and SEN

Bolger writes about steel flow rate and its relationship with the stoppers lift position. To determine this relationship, there have to be a calculation of the open gap between stopper and nozzle seat as a function of stopper lift. The main task in his report is to detect and minimise clogging, which should be of relevance in this report due to the fact that clogging leads to a disturbance of the flow.

9.1.2 Calculation of lift angle

As earlier been discussed, the connection of the stopper rod and nozzle seat can be approximated with a valve. Bolger [6] and Avenberg/ Johansson [7] approximate the gap by the frustum of a right circular cone. To be able to calculate the open area as a function of stopper lift, a lift angle and the line of separation is defined.

Figure 6 in chapter 4.1, shows the cross section of a stopper and a nozzle. The stopper in the physical model has a radius stopper head and the nozzle seat has a constant radius. A refer can be done to Bolger and a calculation of the lift angle can thereby be made.

$$\alpha = \arctan\left(\frac{\sqrt{(Rs+Rh)^2 - \left(Rs+\frac{Db}{2}\right)^2} + l}{Rs+\frac{Db}{2}}\right) \qquad \textbf{(A3)}$$

This equation can be explained by some definitions of the stopper and nozzle dimensions. A triangle is schematically inserted into the system to better explain this relationship, figure A1.

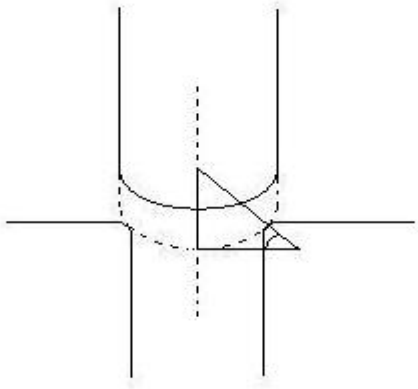

Figure A 1. A lift angle can be calculated between stopper head and seat of the submerged entry nozzle.

The inserted triangle in figure A1 is lifted out of the system and its sides are defined when the stopper is closed, Figure A2.

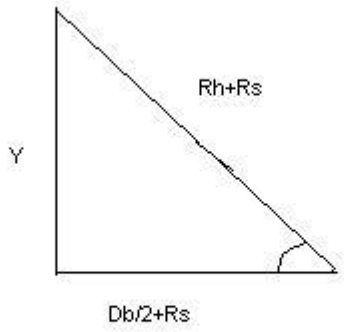

Figure A 2. Triangle from figure 14 with defined sides to be able to calculate the closed stoppers lift angle, which refers to the right corner of the triangle in the figure

Db= Diameter of SEN bore
Rh= Radius of stopper head
Rs= Radius of SEN seat
l= Stopper lift
α= Angle between head to seat and horizontal, in the right corner in figure 15

A definition of the closed stoppers lift angle will now follow, based on the named sides of the triangle in figure A2;

$$\tan\alpha = \frac{Y}{\left(Rs + \frac{Db}{2}\right)} \quad \textbf{(A4)}$$

$$Y = \sqrt{(Rh + Rs)^2 - \left(Rs + \frac{Db}{2}\right)^2} \quad \textbf{(A5)}$$

The expression of equation (A5) can be inserted into equation (A4) and the expression for α, when the stopper is closed, will be;

$$\tan\alpha = \frac{\sqrt{(Rh + Rs)^2 - \left(Rs + \frac{Db}{2}\right)^2}}{\left(Rs + \frac{Db}{2}\right)} \quad \textbf{(A6)}$$

As soon as the stopper opens, molten metal will start to flow through the system. The angle α is widened, and thereby the cross section of the gap. Figure A3 shows schematically how the lift angle is increases.

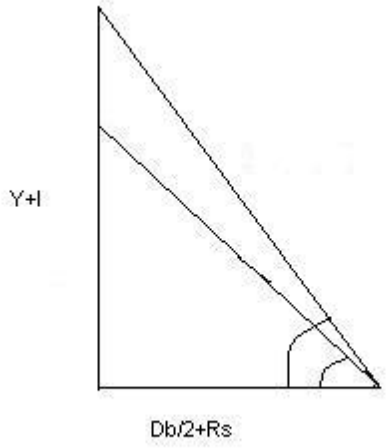

Figure A 3. The triangle in figure 15 changes as soon as the stopper opens. This relationship can be explained as a function of stopper lift

Angle α is widened and is now taken the expression;

$$\tan\alpha = \frac{Y + l}{\left(Rs + \frac{Db}{2}\right)} \qquad \textbf{(A7)}$$

The relationship for Y in equation (A5) will still be valid and is inserted to (A7).

$$\tan\alpha = \frac{\sqrt{(Rh + Rs)^2 - \left(Rs + \frac{Db}{2}\right)^2} + l}{\left(Rs + \frac{Db}{2}\right)} \qquad \textbf{(A8)}$$

With this relationship, it is understandable that changing of the angle only depends of the stoppers position, i.e. when the stopper changes from position *Y* until it reaches position *Y+l*, since all the other measurements of the geometries in the stopper head and nozzle seat are constants.

The physical model has values of stopper radius, 0.060 m, bore diameter, 0.070 m, and radius at the seat of the submerged entry nozzle, 0.050 m. Figure A4 represents lift angle as a function of stopper lift, when a variation of the stopper lift occurs from 0 to 65 mm. Notice that equation (A6) represents the stoppers starting position and a minimum lift angle will thereby be restricted to 39.4 degrees.

The reason for the numerical values of the stopper lift position is that a restriction is inserted at 65 mm in the physical model.

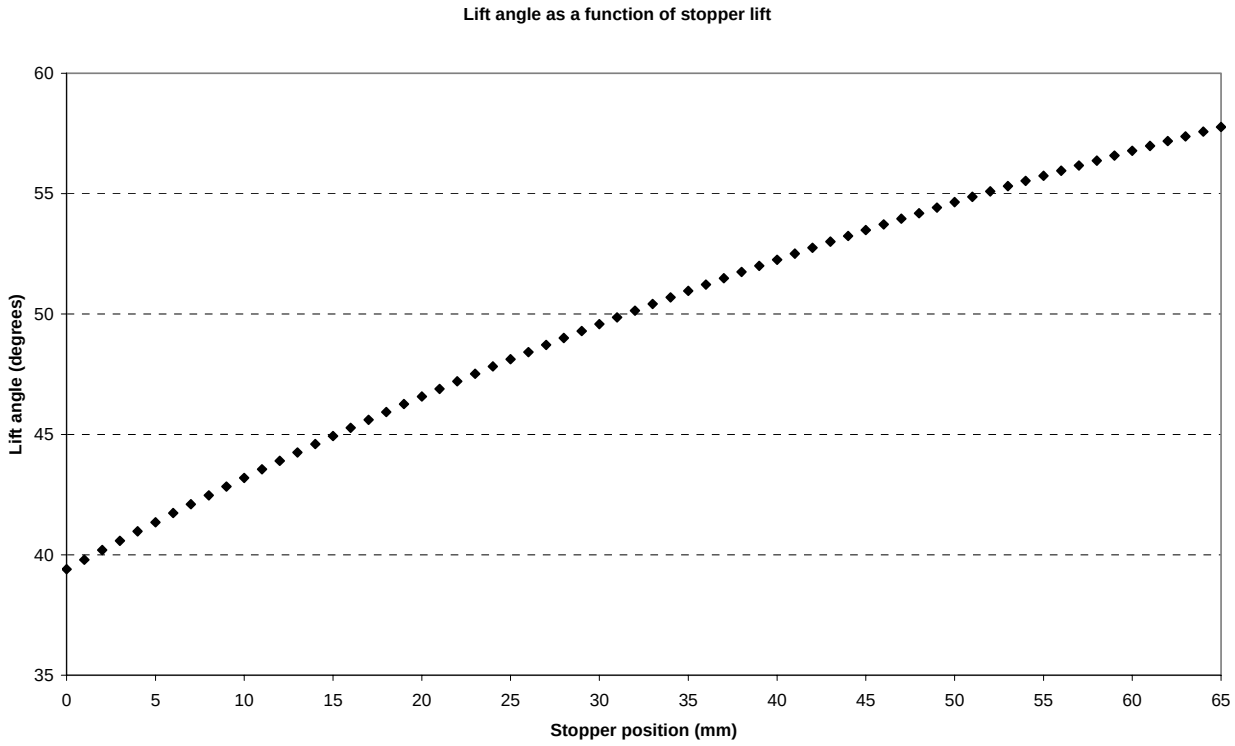

Figure A 4. Lift angle as a function of stopper lift.

9.1.3 Line of separation

Bolger [6] describes the line of separation between stopper and seat by the following formula;

$$s = \frac{\sqrt{(Rh + Rs)^2 - \left(Rs + \frac{Db}{2}\right)^2} + l}{\sin\alpha} \qquad \textbf{(A9)}$$

I will define the formula and represent s as the hypotenuse an thereby;

$$s = x + Rh + Rs \qquad \textbf{(A10)}$$

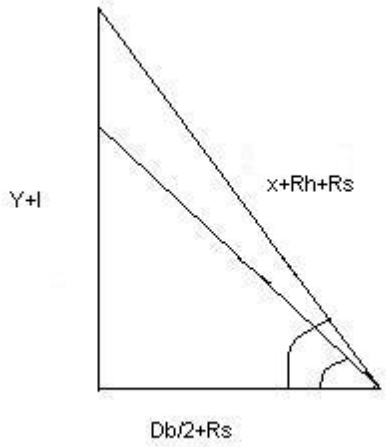

Figure A 5. The line of separation between stopper and nozzle seat can be described by the changing hypotenuse, which will be dependent on the lift angle and stopper lift

From equation (A5), we know the expression for Y and through definition;

$$\sin\alpha = \frac{Y+l}{x+Rh+Rs} = \frac{\sqrt{(Rh+Rs)^2 - \left(Rs+\frac{Db}{2}\right)^2} + l}{x+Rh+Rs} \qquad \textbf{(A11)}$$

Consider revising;

$$s = x+Rh+Rs = \frac{\sqrt{(Rh+Rs)^2 - \left(Rs+\frac{Db}{2}\right)^2} + l}{\sin\alpha} \qquad \textbf{(A12)}$$

When *l* is equal to zero, *x* will also refer to zero. This equation also agrees with Bolger [6]. The line of separation between stopper head and nozzle seat are schematically shown in figure A6 as a function of stopper position. At a closed stopper position, line s will be equal to the sum of stopper head radius and nozzle seat radius, 110 millimetres.

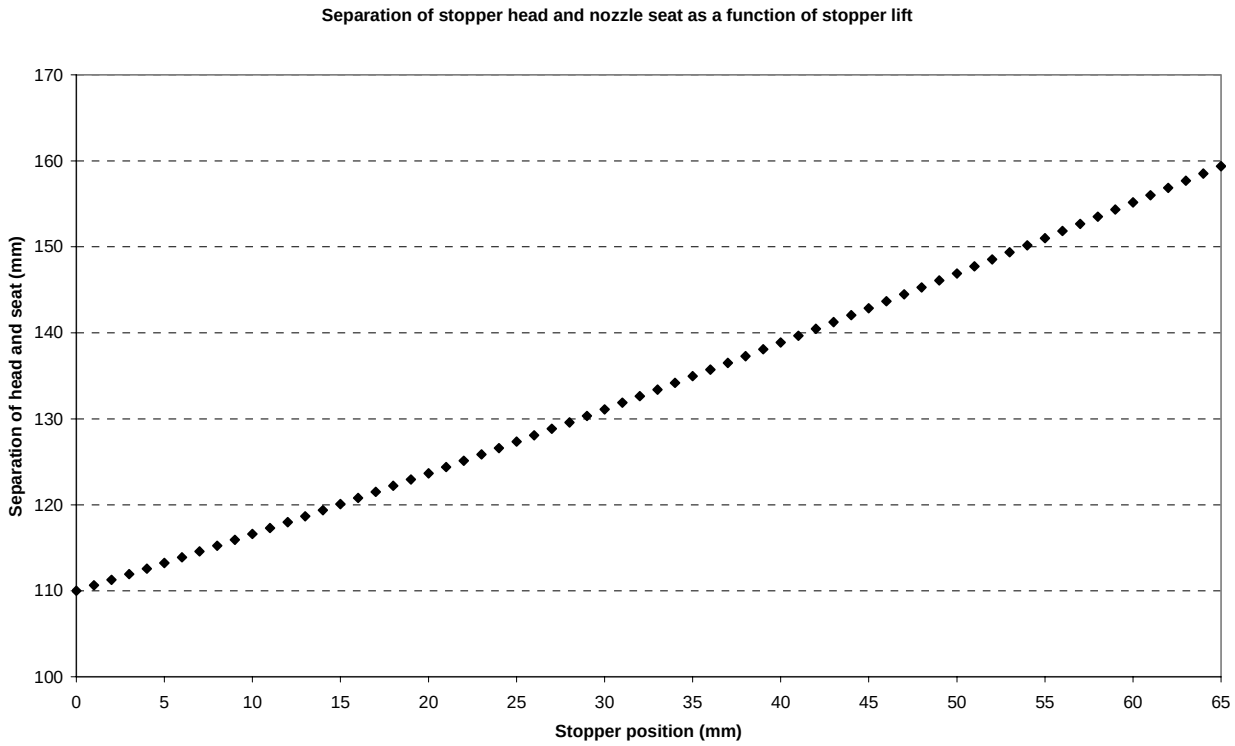

Figure A 6. The line of separation between stopper head and nozzle seat is described as a function of stopper lift position

9.1.4 Calculation of open area as a function of stopper lift

The opening between stopper head and nozzle seat can be expressed by the frustum of a right circular cone in terms of lift angle, line of separation and stopper position [6-7].
The lateral area of the frustum of a right circular cone can be calculated by the general formula;

$$A = \pi * a * (r + R) \qquad \textbf{(A13)}$$

A= lateral area
a= slant height
r= upper radius
R= lower radius

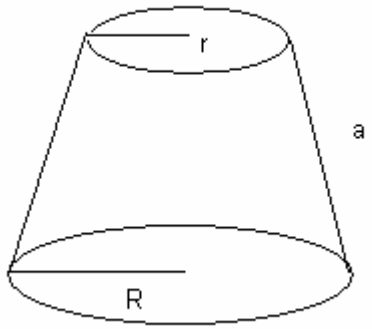

Figure A 7. Definition of the sides in the frustum of a right circular cone, which is approximated with the opening of the cross sectional area between the stopper head and the seat of the submerged entry nozzle

The upper radius of the cone will be described as a function of lift angle;

$$r = Rh * \cos\alpha \quad \textbf{(A14)}$$

The lower radius can also be described as a function of lift angle;

$$R = (a + Rh) * \cos\alpha \quad \textbf{(A15)}$$

$$A = \pi * a * \left(Rh * \cos\alpha + a * \cos\alpha\right) \quad \textbf{(A16)}$$

Where the slant height, a, refers to

$$a = s - Rh \quad \textbf{(A17)}$$

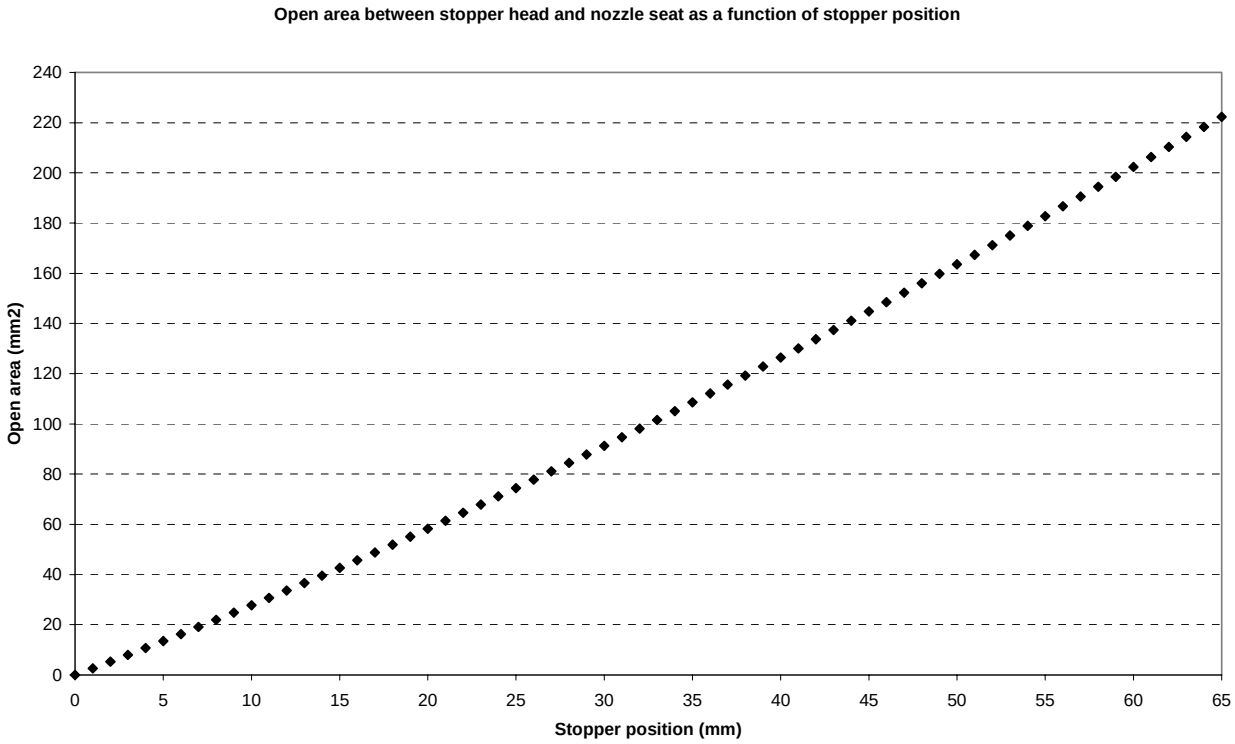

Figure A 8. Open area, mm^2, between stopper and SEN seat as a function of stopper lift (mm).

With the calculated expression of the open area, equation (A16), we know how the open area changes with the stoppers position and we can thereby theoretical decide the flow of steel through the valve.

It should be mentioned that the calculated area in this report coincides with the expression of the area calculated in the report of Avenberg /Johansson [7] but not with the expression for the area in the report made of Bolger [6].

9.2 Definition of flow

It has been told that flow in tundish is generally turbulent and flow in mould should be laminar to not disturb stability at the meniscus. Reynolds number is of vital importance in the study of fluid flow. Re less than 2000 often denotes laminar flow while Re more than 4000 is turbulent flow. Between this numbers, there is a region of transition from laminar to turbulent flow [12].

9.2.1 Flow in tundish

Flow through the submerged entry nozzle is gravity driven by the difference between the liquid steel levels in the tundish and in the mould. Flow rate or casting speed depends upon the tundish bath depth, the regulation and other flow characteristics inside the nozzle. Both clogging and argon injection may greatly affect the flow pattern in the nozzle and subsequently in the mould, by altering the flow rate and flow transients and thereby cause quality problems [10].

The stopper system regulates the flow from tundish to the entry nozzle which finally reaches the mould. The flow from tundish into the casting nozzle can be described in two steps;

1. Liquid metal is passing a converging duct, a nozzle, as long as the area contracts. This is valid from a fully open stopper until the stopper approaches its minimum value

2. Liquid metal passes the minimum opening and flows through an expanding duct, a diffuser. This is valid from the stoppers minimum value until the stopper is fully open.

When the stopper reaches a certain value, it will lose its regulating ability and the flow into the casting nozzle will only depend on the diameter of the pipe. A convergent flow occurs when in a nozzle and a divergent in the case of a diffuser. In the case of a non regulating device, there will only be a contraction when the area decreases at the entrance to the casting nozzle.

The rate of flow of any fluid through an orifice or nozzle, neglecting the velocity of approach, is derived from the equation of continuity [18] and may be expressed by;

$$q = C_D * A * \sqrt{2 * g * h_L} \quad \textbf{(A18)}$$

C_D= Flow coefficient
A= Cross sectional area (m^2)
g= Acceleration due to gravity (m/s^2)
h_L= Head loss (m)

The velocity of approach may have a considerable effect on the quantity that discharges through a nozzle or an orifice. There is a factor correction for the velocity of approach;

$$\frac{1}{1-\beta^4} \quad \textbf{(A19)}$$

And this equation can be incorporated into equation (25)

$$q = \frac{C_D * A}{\sqrt{1-\beta^4}} \sqrt{2 * g * h_L} \quad \textbf{(A20)}$$

β=The ratio of orifice or throat diameter to inlet diameter.

A new parameter, *C,* is introduced and defined as the flow coefficient. The use of this coefficient eliminates the necessity of calculating the velocity of approach. The value of C depends on Reynolds number and on the ratio of *β.*

$$C = \frac{C_D}{\sqrt{1-\beta^4}} \quad \textbf{(A21)}$$

The pressure drop that occurs over the valve, is dependent of head loss and is described by equation (29)

$$\Delta P = \rho * g * h_L \quad \textbf{(A22)}$$

Inserting equation (29) and (30) into equation (27)

$$q = C * A * \sqrt{2 * g * h_L} = C * A * \sqrt{\frac{2 * \Delta P}{\rho}} \quad \textbf{(A23)}$$

ΔP= Difference in pressure in the key locations (Pa)
ρ= Density of the metal (kg/m^3)

9.2.2 Flow in casting nozzle

Flow in a pipe can be calculated from the pressure drop that occurs in it. This is dependent of the head loss in the pipe and can also be calculated from equation (A22).

Head loss can further be expressed by;

$$h_L = \frac{f * l * v^2}{2 * d * g} \quad \textbf{(A24)}$$

Velocity can be calculated according to the well known relationship;

$$v^2 = \frac{q^2}{A^2} \quad \textbf{(A25)}$$

Equation (A24) and (A25) can now be inserted to equation (A22) and be considered as;

$$\Delta P = \frac{\rho * g * f * l * v^2}{2 * g * d} = \frac{f * l * \rho * q^2}{d * 2 * A^2} \quad \textbf{(A26)}$$

This equation is known as the Darcy equation and is valid for laminar and turbulent flow of any liquid in a pipe [18].

f= Friction factor[2]
l=Length under consideration (m)
v=Velocity (m/s)
d=Diameter of pipe (m)
g=Acceleration due to gravity (m/s^2)
q=Volumetric flow (m^3/s)
A=Cross section of pipe (m^2)

[2] For laminar flow conditions, the friction factor is a direct mathematical function of Reynolds number and is calculated by 64/Re. [18]

9.2.3 Flow in mould

In the introduction to this chapter, it was told that the flow the mould should be laminar to ensure meniscus stability and thereby a better quality of the cast material.

The flow into the mould can also be derived from the equation of continuity;

$$q = \pi * r^2 * \sqrt{2 * g * h_L} = \pi * d^2 \sqrt{\frac{\Delta P}{8 * \rho}} \quad \textbf{(A27)}$$

q=Volumetric flow into mould (m^3/s)
r=Radius of submerged entry nozzle (m)
d=Diameter of submerged entry nozzle (m^2)
g=acceleration due to gravity (m/s^2)
ΔP=Pressuredifference (N/m^2)
ρ=Density of metal (kg/m^3)

9.2.4 Pressure and pressure relations

In continuous casting, there are always discussion about pressure and flow. Some basic expressions of pressure will thereby be explained, before the discussion goes deeper into pressure expressions. Figure 22 views relations of different kinds of pressure conditions.

Pressure is a force exerted by a fluid per unit area. The actual pressure in a position is called the absolute pressure and is measured relative to absolute vacuum. Most pressure measuring devices, however, are calibrated to read zero in the atmosphere and they indicate thereby the difference between the absolute pressure and the local atmospheric pressure. This pressure is referred to as gage pressure.

Pressures below atmospheric pressure are called vacuum pressures and are measured by vacuum gages which indicate the difference between the atmospheric pressure and the absolute pressure. Absolute, gage and vacuum pressure are all positive quantities. It will though be referred to negative pressure in this text. So called negative pressures are the referred to as negative gauge pressures or vacuum.

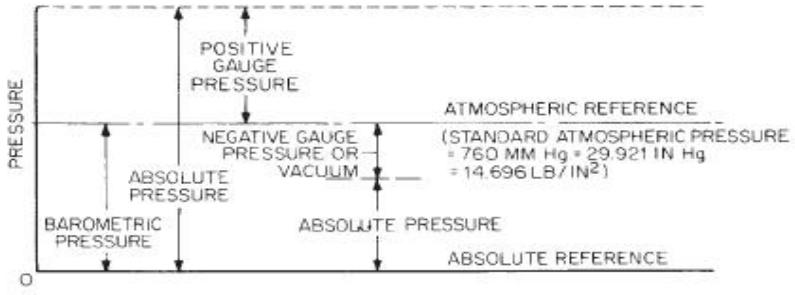

Figure A 9. Relation between different kinds of pressures

As metal flows through the regulating device between tundish and casting nozzle, there will be a sudden contraction followed by an enlargement of the area as the metal passes through the valve. Suzuki [5] explains this sudden decrease in pressure as a source of oxidation of the aluminium in molten steel, due to the fact that pressure is reduced below atmospheric and air is possibly permeated through the refractory. He found that the negative pressure was a generated just below a sliding gate between tundish and submerged entry nozzle. This would refer to the place where the area is enlarged and would thereby be similar in our physical model.

Bai and Thomas [10] Shows that the partial vacuum in the nozzle could be reduced by increasing the gas flow rate or pressurising the nozzle. The minimum pressure inside the nozzle is affected by argon injection, tundish bath depth, casting speed, gate opening and clogging. Predicting when a partial vacuum condition exists and choosing conditions to avoid it is one way to prevent this potential source of reoxidation products and the associated clogging and quality problems.

Heaslip [9] shows in a water modelling with stopper rod control of the flow, that gas flow rates less than or equal to 0,75 ft^3/min a reduced pressure can be seen with an increased casting rate and a constant gas flow rate. Increasing the gas flow rate, however, increases the pressure at the injection site at the end of the tube located in the centre of the hollow stopper rod [9].

Bolger [6] derives Bernoulli's theorem, chapter 4.4.3, and describes the pressure distribution in five different points according to figure 23. The pressure in some key locations can according to Bolger be calculated by the following expressions in equation (36) to (40).

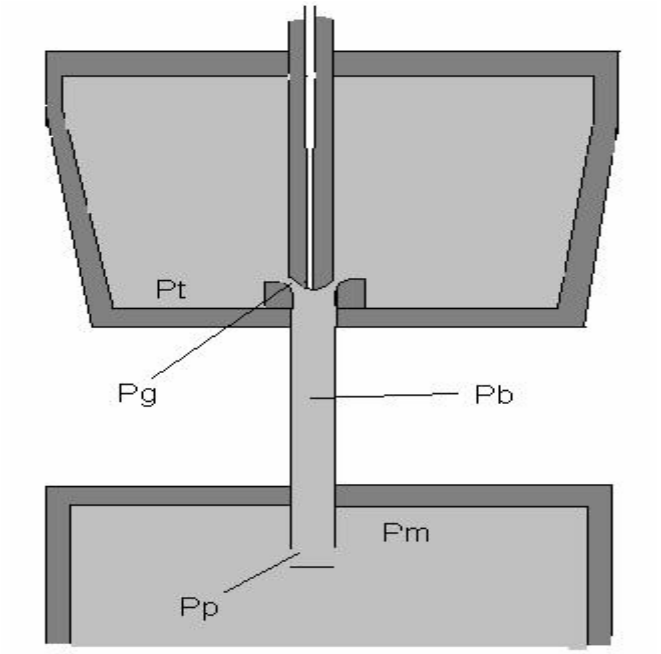

Figure A 10. Pressure distribution in tundish and mould can be derived from Bernoulli's equation due to different locations

Pressure in tundish is a function of height and can be explained by;

$$P_T = \rho * g * h_T \quad \textbf{(A28)}$$

Travelling further down in the system, to the gap between Stopper and seat of the submerged entry nozzle, gives us a new expression for the pressure.

$$P_G = P_T + \rho * g * l + \frac{Q^2}{2 * \rho * A_G^2} \quad \textbf{(A29)}$$

Bore of submerged entry nozzle below stopper head (B)

$$P_B = P_G + \rho * g * (h_B - h_G) + (1 - f) * \frac{Q^2}{2 * \rho}\left(\frac{1}{A_B^2} - \frac{1}{A_G^2}\right) \quad \textbf{(A30)}$$

Port of submerged entry nozzle (P)

$$P_P = P_B + \rho * g * (h_B - h_P) \quad \textbf{(A31)}$$

And finally, the mould (M)

$$P_M = P_P + \rho * g * (h_M - h_P) + (1 - f) * \frac{Q^2}{2 * \rho} \left(\frac{1}{A_M^2} - \frac{1}{A_P^2} \right) \quad \textbf{(A32)}$$

A notice that should be made is that Bernoulli's theorem is a calculation based on laminar flow. The flow in the physical model is determined by an indirect method. A discussion and calculation based on Reynolds number at these flows will follow in appendix B.

10 Appendix B

Reynolds number can be calculated for the simulation of single phase flow in continuous casting. A theoretically comparison can be made with steel.

Calculations based on the volumetric flow in the physical model were done according to table B1. The diameter of the casting nozzle is 0.07 m and the hydraulically diameter for the mould is calculated in equation (B1), and Reynolds number could thereby be calculated in the submerged entry nozzle and in the mould, table B1.

$$d_h = \frac{4 * A}{s} \qquad \textbf{(B1)}$$

d_h= hydraulically diameter
A= cross section
s= circumference of the mould

The hydraulically diameter of the mould will be;

$$d_h = \frac{4 * 0{,}2 * 0{,}8}{0{,}2 * 2 + 0{,}8 * 2} = 0{,}32m$$

$$\mathrm{Re}_{nozzle} = \frac{\rho * u * d_{nozzle}}{\mu}$$

$$\mathrm{Re}_{mould} = \frac{\rho * u * d_h}{\mu}$$

Table B1 shows the calculated Reynolds number in the nozzle and the mould at the actual pumping velocities at the experiments.

Table B1. Calculated Reynolds number in entry nozzle and mould

Pumping velocity (rpm)	Velocity in nozzle (m/min)	Reynolds number in nozzle	Casting velocity (m/min)	Reynolds number in mould
750	12.63	71427	0,30	7756
800	16.42	92861	0,39	10083
850	20.63	116670	0,49	12668
900	25.69	145286	0,61	15770
950	30.74	173846	0,73	18873
1000	36.21	204780	0,86	22234
1020	38.32	216714	0,91	23526
1050	42.11	238148	1,00	25853
1100	48.43	273889	1,15	29731

It can be seen that Reynolds number is very high due to the high density and the low viscosity of the alloy. A comparison with steel is made in table B2 for the velocities in the nozzle and the mould. The viscosity of liquid iron is 6.44 mPas [26] and the density is 7800 kg/m^3 [25].

Table B2. Calculated Reynolds number in entry nozzle and mould for steel

Pumping velocity (rpm)	Velocity in nozzle (m/min)	Reynolds number in nozzle	Casting velocity (m/min)	Reynolds number in mould
750	12.63	17958	0,30	1950
800	16.42	23347	0,39	2535
850	20.63	29333	0,49	3185
900	25.69	36528	0,61	3965
950	30.74	43708	0,73	4745
1000	36.21	51486	0,86	5590
1020	38.32	54486	0,91	5915
1050	42.11	59875	1,00	6500
1100	48.43	68861	1,15	7475

Reynolds number is lower in the mould than in the casting nozzle for all pumping velocities. Thus, all pumping velocities at these experiments would show laminar flow in the mould if steel would be used.

11 Appendix C

The following figures, *C*1-*C*8, views mean signal intensity as a function of frequency for a frequency spectrum from zero to 30 Hz. Each of the figures refers to a specific velocity of the pump and thereby a specific volumetric flow in the model. Each measurement, and thereby each diagram, shows the signal from both the casting nozzle and the engine of the pump. The mean signal intensity is located at the *y*-axis and the frequency can be studied at the *x*-axis.

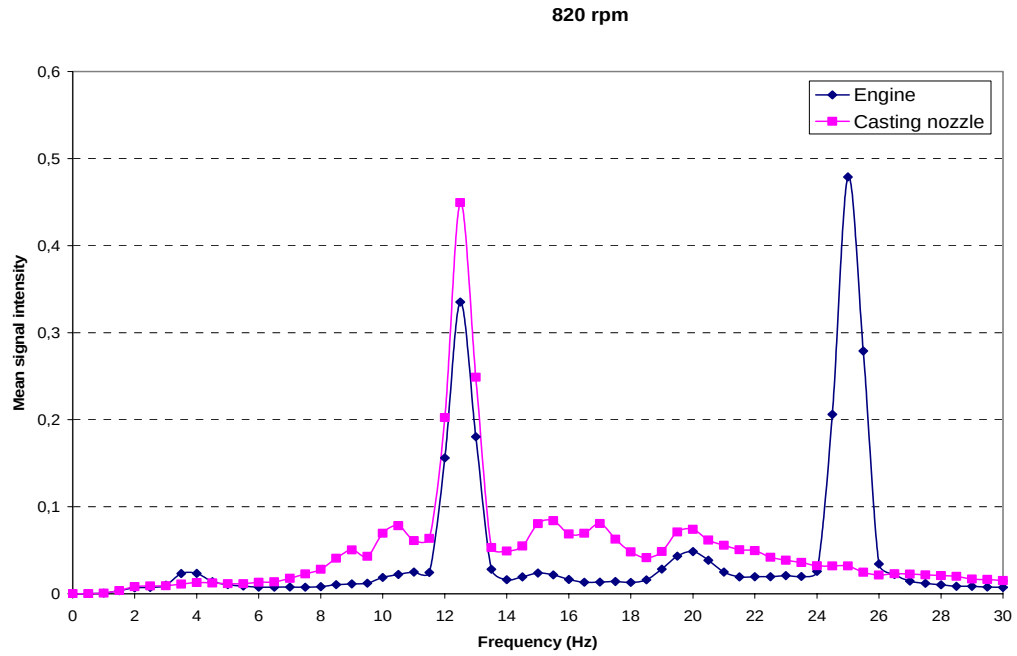

Figure C 11. Mean signal intensity for a frequency spectrum of 0-30 Hz at a pumping velocity of 820 rpm

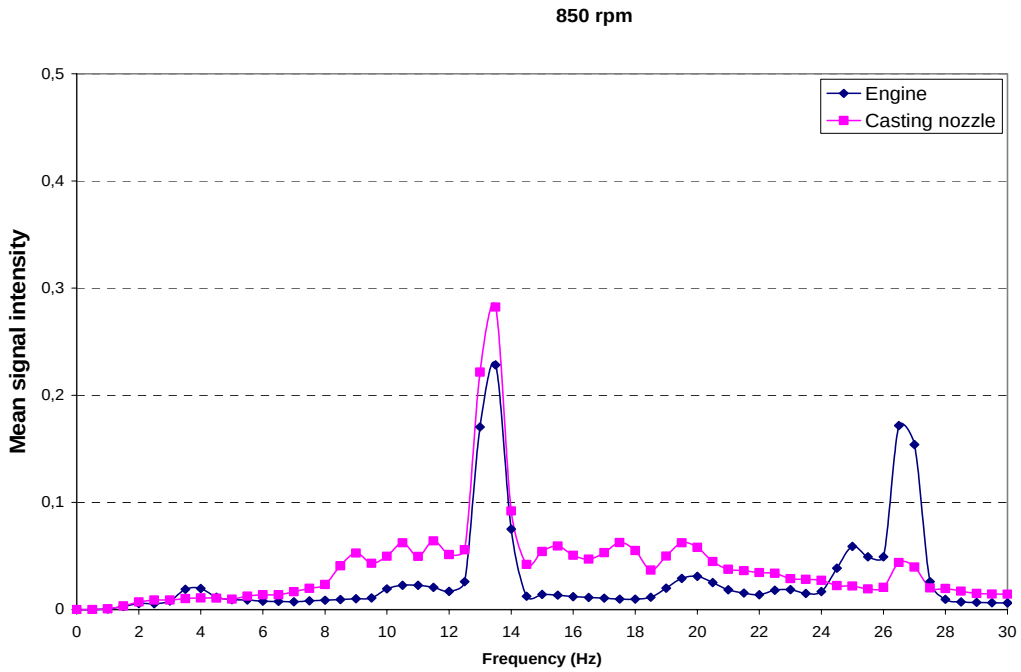

Figure C 12. Mean signal intensity for a frequency spectrum of 0-30 Hz at a pumping velocity of 850 rpm

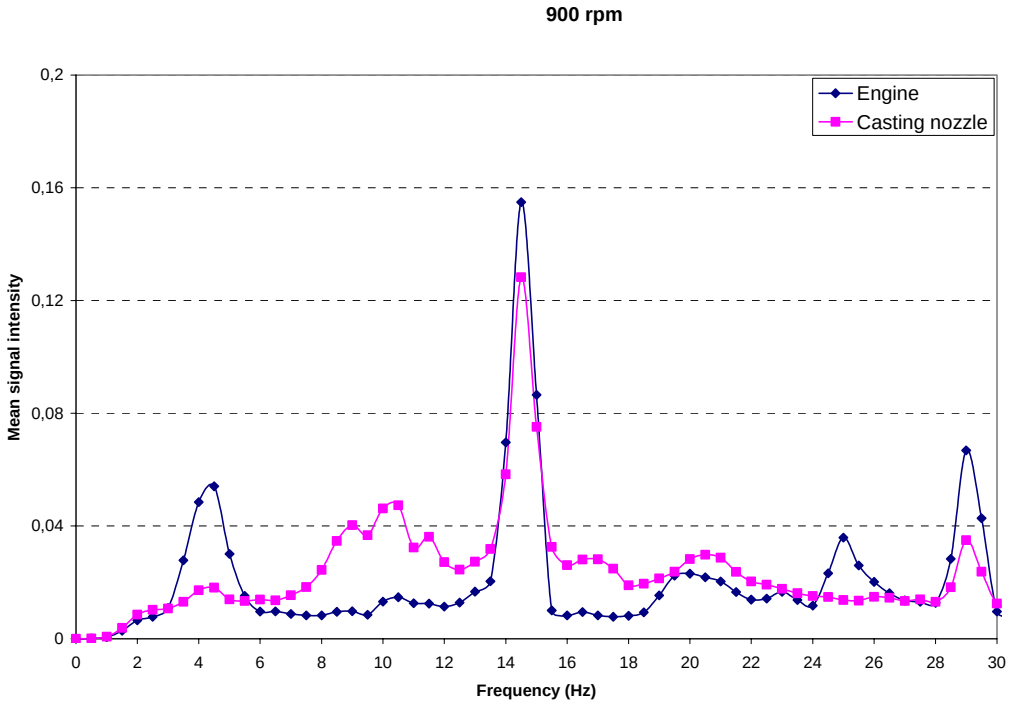

Figure C 13. Mean signal intensity for a frequency spectrum of 0-30 Hz at a pumping velocity of 900 rpm

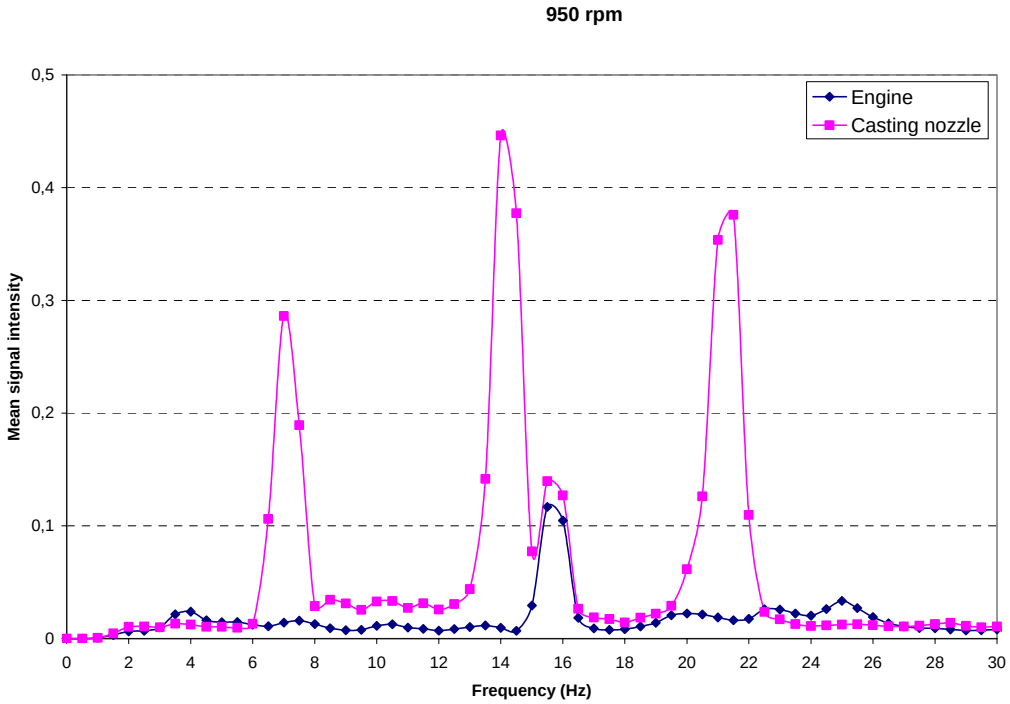

Figure C 14. Mean signal intensity for a frequency spectrum of 0-30 Hz at a pumping velocity of 950 rpm

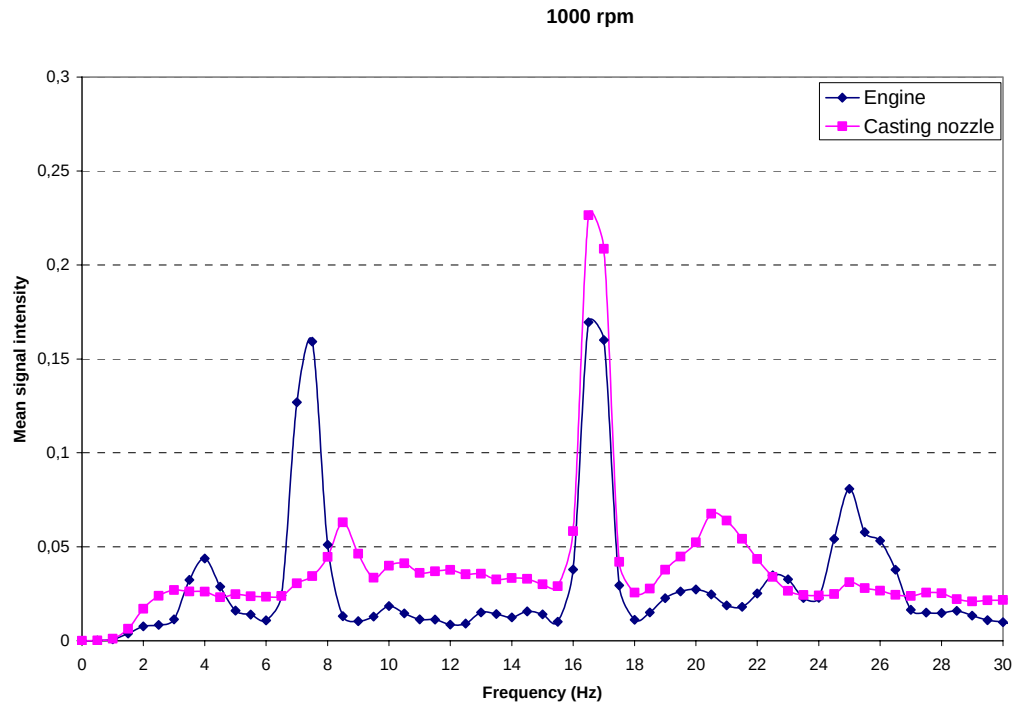

Figure C 15. Mean signal intensity for a frequency spectrum of 0-30 Hz at a pumping velocity of 1000 rpm

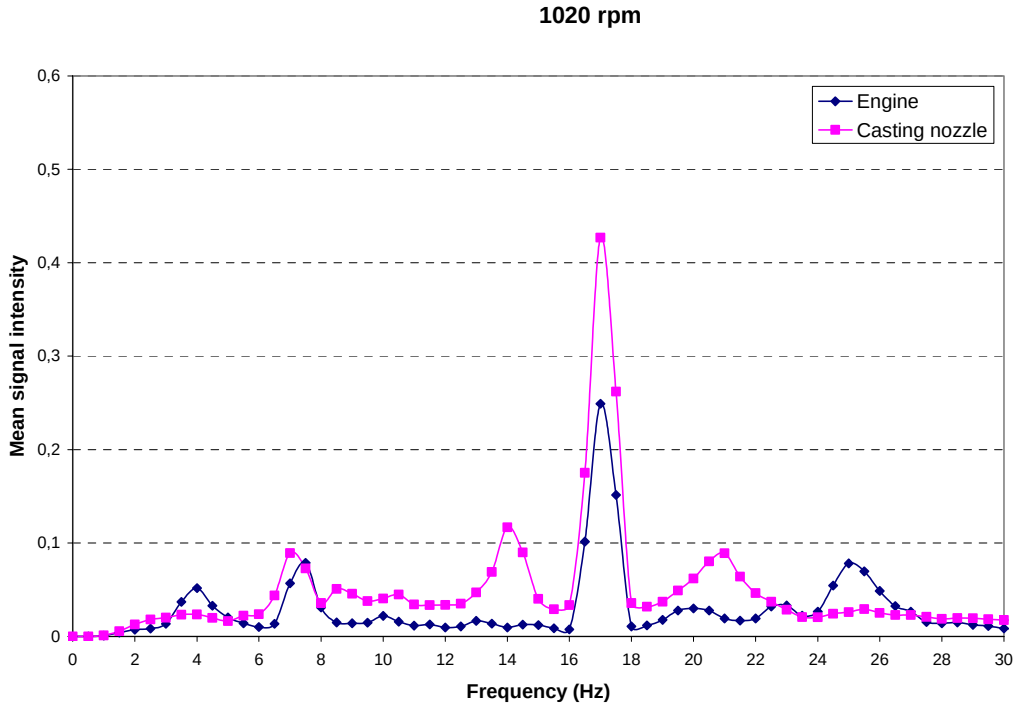

Figure C 16. Mean signal intensity for a frequency spectrum of 0-30 Hz at a pumping velocity of 1020 rpm

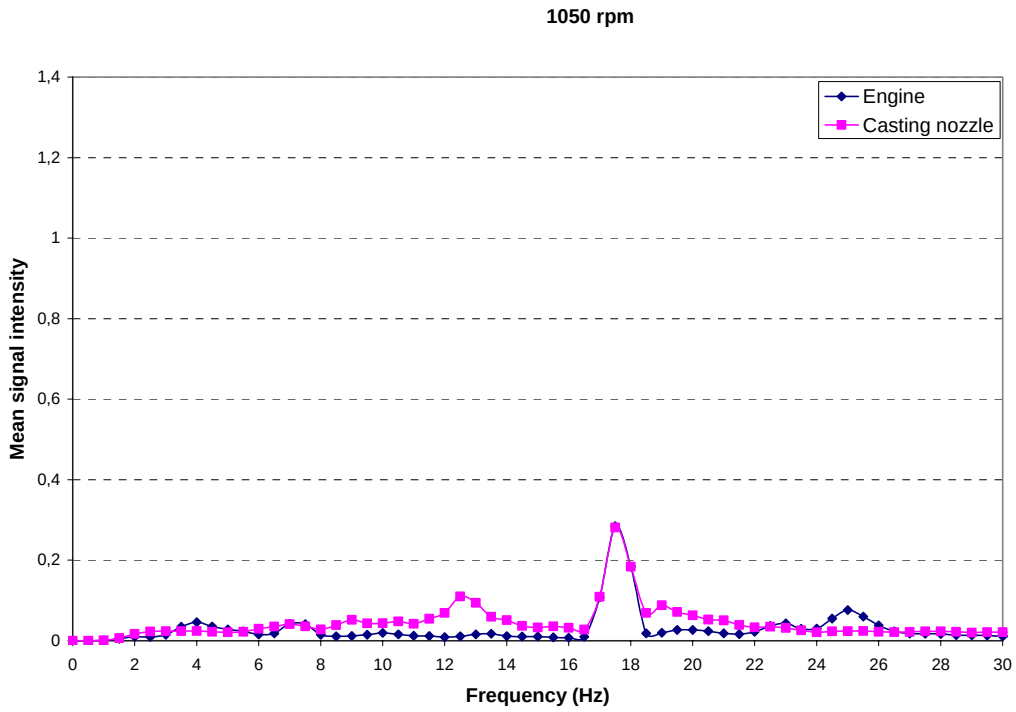

Figure C 17. Mean signal intensity for a frequency spectrum of 0-30 Hz at a pumping velocity of 1050 rpm

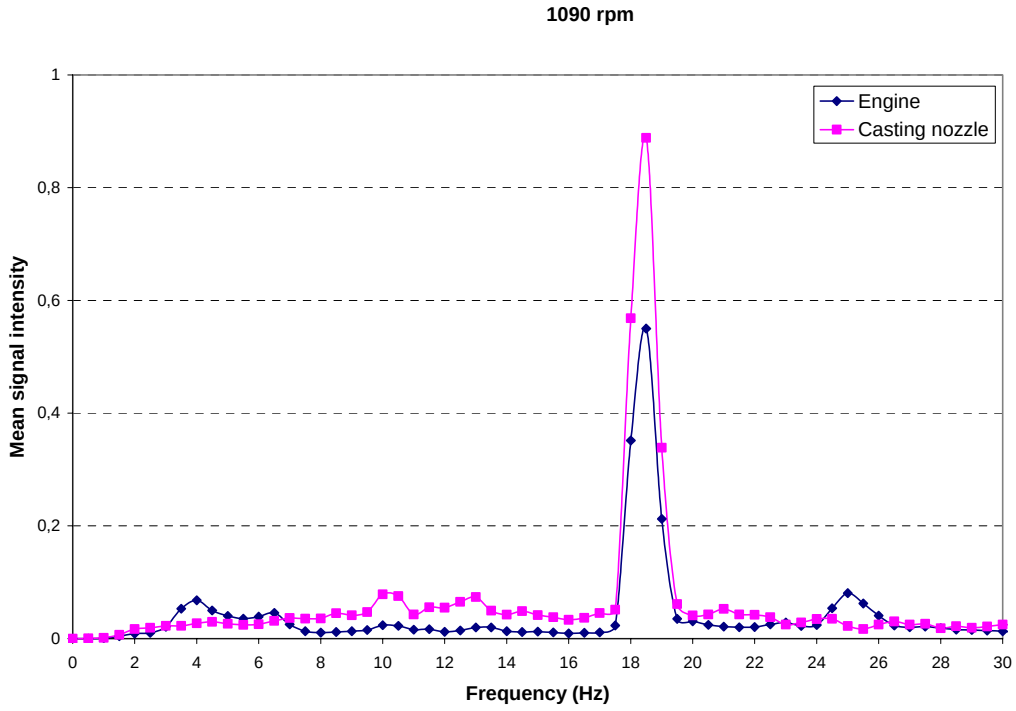

Figure C 18. Mean signal intensity for a frequency spectrum of 0-30 Hz at a pumping velocity of 1090 rpm